

Controls on the distribution and resilience of *Quercus garryana*: ecophysiological evidence of oak's water-limitation tolerance

W. JESSE HAHM ¹, † WILLIAM E. DIETRICH,¹ AND TODD E. DAWSON²

¹Department of Earth and Planetary Science, University of California – Berkeley, Berkeley, California 94720 USA

²Center for Stable Isotope Biogeochemistry, Department of Integrative Biology, University of California – Berkeley, Berkeley, California 94720 USA

Citation: Hahm, W. J., W. E. Dietrich, and T. E. Dawson. 2018. Controls on the distribution and resilience of *Quercus garryana*: ecophysiological evidence of oak's water-limitation tolerance. *Ecosphere* 9(5):e02218. 10.1002/ecs2.2218

Abstract. The composition of forests in Western North America is changing. The decline in the shade-intolerant Oregon white oak (*Quercus garryana* var. *garryana*) is attributed to increased competition with the tall-growing Douglas fir (*Pseudotsuga menziesii* var. *menziesii*) as a result of widespread fire exclusion. In a warmer, drier future, both species will experience increased water stress, and their distribution will depend on ecophysiological adaptations to water limitation, of which little is known for *Q. garryana*. Here, we report a suite of new ecophysiological observations to better understand the oak's water-limitation tolerance, in order to predict its fate in a changing climate. Our study site in the Central Belt of the Franciscan Formation in the Northern California Coast Ranges receives almost no rain in the leaf-on growing season and has limited subsurface water storage capacity. In spite of low pre-dawn water potentials (Ψ ; to below -3.0 MPa), mature trees maintained high rates of sapflow. Sapflow continued due to a high Ψ gradient (≈ 1.6 MPa on average) at mid-day between shoots and the subsurface (inferred from pre-dawn measurements) throughout the dry season. Depletion and recharge of stored water in stem tissue and leaves helped to sustain transpiration. Leaves experienced low Ψ (below -4 MPa), and declining hydraulic conductance yet remained functional. Pressure–volume curve analyses revealed that the maintenance of positive turgor pressures in leaves at low Ψ may be attributable to dynamic adjustment due to changes in cell wall elasticity. The turgor loss point may be of limited use in delineating ecophysiological limits to growth and reproduction, as transpiration and apparently normal physiological behavior continued after pre-dawn water potentials declined below turgor loss limits inferred from rehydrated leaves. These findings indicate that *Q. garryana* is a water-limitation-tolerant tree species that maintains hydraulic function as subsurface water supply and atmospheric demand conditions exceed the ranges at which *P. menziesii* can operate. These observations can be used to explain *Q. garryana*'s extant species range and anticipate its likely resilience in a warmer climate.

Key words: drought; ecophysiology; fire exclusion; Garry Oak; Mediterranean climate; Oregon White Oak; plant–water relations; *Quercus garryana*; sapflow; water potential; water storage; water-limitation tolerance.

Received 20 March 2018; accepted 20 April 2018. Corresponding Editor: Jason B. West.

Copyright: © 2018 The Authors. This is an open access article under the terms of the Creative Commons Attribution License, which permits use, distribution and reproduction in any medium, provided the original work is properly cited.

† **E-mail:** wjhahm@berkeley.edu

INTRODUCTION

The composition and function of ecosystems are undergoing rapid alteration (Foley et al. 2005, Marlon et al. 2008, Loarie et al. 2009). Globally, tree species distributions depend

primarily upon water availability (Holdridge 1947, Woodward 1987), which in turn depends on precipitation patterns, atmospheric demand for water, and, in seasonally dry climates, the capacity of the subsurface to store and release water to terrestrial ecosystems (Jones and

Graham 1993, Anderson et al. 1995, Porporato et al. 2001). Warm dry periods can result in widespread mortality: In the state of California alone, the most recent drought resulted in the death of more than one hundred million trees (Asner et al. 2016, US Forest Service 2016), a vivid example of the limits of ecosystems to climate perturbations. These types of events have spurred research into understanding plant response to changing climate, with a particular emphasis on water-use strategies and species-level traits that prolong functioning in drought (McDowell et al. 2008, Allen et al. 2010, Bartlett et al. 2012 and West et al. 2012).

Alteration of natural and historic fire regimes can interact with water limitation. In western North America, for instance, fire-intolerant conifers (primarily coast Douglas Fir, *Pseudotsuga menziesii* var. *menziesii*) have encroached upon oak habitat in the wake of post-Euro-American-contact fire exclusion—that is, the cessation of intentional burning and the active suppression of naturally ignited fires (Sprague and Hansen 1946, Devine and Harrington 2006, Pellatt and Gedalof 2014). The dominant oak along most of the Pacific west coastal mountains, *Quercus garryana* Dougl. ex. Hook. var. *garryana* (Oregon White or Garry oak), has experienced radical habitat loss yet has received relatively little research on its ecophysiology within its ecological context (exceptions include Phillips et al. 2003a, Davis 2005, Kelly 2016, and Merz et al. 2017). This information gap hinders our ability to predict and manage the oak's fate as climate warming accelerates (Smith et al. 2015). The success of physiologically based mechanistic models of species-level sensitivity to climatic and subsurface water status relies on accurate parameterization of how key plant traits respond in concert to water limitation. Although individual traits have been studied (Phillips et al. 2003b, Davis 2005, Meinzer et al. 2005, 2016, Johnson et al. 2009, 2012, Merz et al. 2017), the collective water relations of wild, mature *Q. garryana* have not been documented.

In seasonally dry Mediterranean climates, water availability is generally out of phase with solar energy supply. Plants develop strategies and traits to obtain water as the subsurface progressively dries. As turgor is generally required for hydraulic function, there is a tendency for

species with low turgor loss points (TLPs) to be water-limitation tolerant, and plants with low TLP tend to be found in more xeric habitats (Bartlett et al. 2012, Meinzer et al. 2016). Significant variability in the TLP exists among co-occurring or even sympatric species, however, and seasonal and daily plasticity of osmotic potential or cell wall elasticity can prolong turgor loss (Joly and Zaerr 1987, Dawson and Bliss 1989, Marshall and Dumbroff 1999). This indicates that the TLP alone is insufficient to adequately characterize a species' sensitivity to water limitation for many predictive purposes and highlights the need for a more comprehensive understanding of individual species' water-use strategies to predict resilience to climate change and inform management decisions.

Quercus garryana range

Within *Q. garryana*'s naturally occurring range (Fig. 1), annual average precipitation increases more than tenfold, from <170 mm in the Tehachapi Mountains of southern California to >2000 mm in the Cascades of Oregon (Stein 1990). *Quercus garryana* has the largest north-south range of any west-coast oak and is the only native oak in Washington and British Columbia and the principal native oak in Oregon. At the northern end of *Q. garryana*'s range, oak woodlands appear to be concentrated in the relatively xeric microclimates induced by orographic shielding (Pellatt and Gedalof 2014). Such biogeographic associations and findings from Franklin and Dyrness (1973) led Minore (1979) to rank *Q. garryana* as the most drought-tolerant common tree species in the Pacific Northwest. *Quercus garryana*'s competitive advantage over faster-growing species in the wetter parts of its range derives in large part due to its adaptation to fire.

Quercus garryana and fire

Conservationists predict that status quo fire exclusion in western North America will continue to result in takeover of *Q. garryana* woodlands and savanna by *P. menziesii* (Reed and Sugihara 1987). This prediction is based on the assumption that throughout their mutual range (Fig. 1) *Pseudotsuga menziesii* can outcompete *Q. garryana* in fire-excluded areas, and the observation that many *Q. garryana* woodlands and

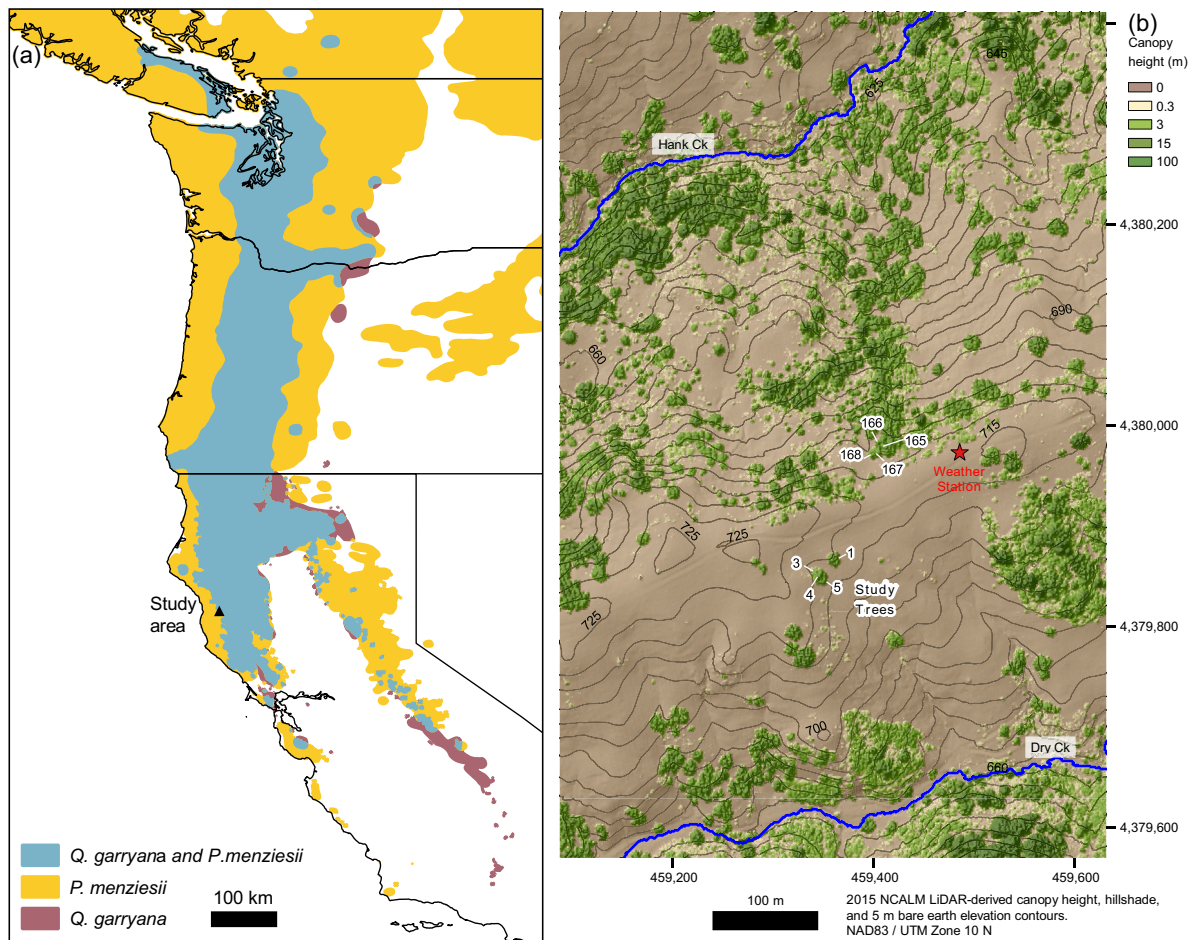


Fig. 1. (a) Map showing distribution of *Quercus garryana* and *Pseudotsuga menziesii* in western North America and study area (black triangle). The *Q. garryana* range is almost entirely subsumed by *P. menziesii*, except at its western- and southern-most margins. Range maps were generated from the union of Little (1971) shapefiles provided by the USGS and scanned, georeferenced, and digitized maps by Griffin and Critchfield (1972) of the state of California, which include smaller, geographically isolated populations at higher spatial resolution. Study area map (b) created from semi-transparent canopy height raster draped over hillshade derived from first return elevations. Elevation contour labels in meters above sea level; white-outlined numbers show the location of study trees (see Table 1).

savannas persisted through the Holocene primarily due to the role of fire, whether anthropogenic or naturally ignited (Devine and Harrington 2006, Pellatt and Gedalof 2014).

Two centuries of fire exclusion, after millennia of intentional burning that promoted oak woodlands and savanna to conifer habitat on the west coast (Cole 1977, Barnhart et al. 1996, Thysell and Carey 2001, Sugihara et al. 2006, Christy and Alverson 2011, Dunwiddie et al. 2011, Gilligan

and Muir 2011, McCune et al. 2013, Cocking et al. 2015, but see exceptions in Thilenius 1968, Gedalof et al. 2006, McDadi and Hebda 2008). Unlike *Q. garryana*, *P. menziesii* is highly susceptible to fire, particularly when young (Engber and Varner 2012). As firs grow, they become more fire resistant and shade out *Q. garryana*, reducing growth and ultimately resulting in mortality (Devine and Harrington 2006, Gould et al. 2011).

Fire exclusion and the consequent loss of oak savanna and woodland adversely affect

ecosystem biodiversity. *Quercus garryana* savanna and woodland host higher levels of species richness than any other terrestrial habitat in California and coastal British Columbia, including numerous at-risk species (California Department of Forestry 1996, Erickson 1996, Fuchs 2001, Zack et al. 2005, Parks Canada 2006a, b, Pellatt et al. 2015). The great biodiversity in *Q. garryana* savanna and woodland ecosystems—and its disappearance under closed-canopy conifer forests—has prompted numerous managers and conservationists to begin manual conifer removal projects and/or prescribed fire treatments (Hastings et al. 1997). This issue remains at the forefront of conservation efforts along the west coast (Miller 2002, Thompson 2007, Dunwiddie and Bakker 2011).

To explore *Q. garryana*'s susceptibility to climate warming and its ability to compete with *P. menziesii* in a warmer future, we selected a field site in the Coast Ranges of Northern California where locally *Q. garryana* is common. Due to an extremely limited subsurface water storage capacity (Hahm et al. 2017b), the *Q. garryana* stands at our study site are not experiencing invasion by *P. menziesii* (Hahm et al. 2017c). We propose that studying the water relations of *Q. garryana* at this site will inform the water-availability conditions that *Q. garryana* can tolerate but *P. menziesii* cannot. We further explored whether *Q. garryana* is more water-limitation tolerant than *P. menziesii* by comparing the water relations of *Q. garryana* to existing literature on the relatively better-studied *P. menziesii*, including a detailed water-use study in an area of essentially identical climate across a geologic contact where *P. menziesii* is the dominant canopy-emergent species (Link et al. 2014).

We hypothesized that, relative to *P. menziesii*, *Q. garryana* would (1) maintain a gradient between pre-dawn and mid-day Ψ longer into the dry summer growing season, (2) maintain higher late dry-season sapflow, reflecting continued water use and photosynthesis, (3) exhibit a lower leaf *TLP*, and (4) have less vulnerable hydraulic pathways. Our findings support all of these hypotheses. *Quercus garryana* is exceptionally water-limitation tolerant; it maintains sapflow at low water potentials (<-4 MPa in leaves), at times when neighboring *P. menziesii*

exhibit marked declines, and exhibits a lower *TLP* and less vulnerable leaf hydraulic network than *P. menziesii*. These observations, in conjunction with paleo- and modern climate responses of the two species, suggest that extant *Q. garryana* woodlands and savanna will persevere as the west coast of North America continues to warm.

METHODS

Site description

The study site, Sagehorn, is located in the Middle Fork Eel River watershed in the Northern California Coast Ranges and is part of the National Science Foundation-supported Eel River Critical Zone Observatory (Fig. 1). The site is ~25 km east of the Pacific Ocean at 700 m above sea level. This study complements ongoing ecohydrological efforts to understand the influence of subsurface weathering profiles on hydrologic runoff pathways and regional forest distribution (Hahm et al. 2017b), oak water sourcing dynamics as inferred via stable isotopes (Hahm et al. 2017a), dynamic hillslope water storage (Dralle et al., *in press*), and the extent of dry-season wetted stream channels (Lovill et al., *in press*).

Climate, geology, and soils.—The site experiences a Mediterranean climate with hot, dry summers and cool, wet winters. Nearly all of the precipitation falls as rain between November and April. The annual average rainfall is ~1800 mm, and the average temperature is 13.3°C (version M2; PRISM Climate Group, Oregon State University, <http://prism.oregonstate.edu>).

The site lies within the Central belt *mélange*, a chaotic metasedimentary belt of the Franciscan Formation complex (Jayko et al. 1989, McLaughlin et al. 1994), which underlies ~50% of the Eel River watershed (Langenheim et al. 2013). The matrix of the *mélange* is argillaceous and encompasses coherent blocks of greywacke, chert, and minor high-grade metamorphics and ultramafics (Blake and Jones 1974, Cloos 1982). Formerly active earthflows are common at the site, but the study trees are situated close to the local topographic divide, above relict earthflow topography (Fig. 1).

Soils at the site are classified as mollisols (Rittman and Thorson 2001). Near the study trees, a

typically 30 cm thick brown–black organic-rich granular mineral A horizon abruptly overlies a yellow-gray, massive 10–20 cm thick Bt horizon that has a sharp decrease in organic matter content and higher clay content. Below the Bt horizon lies a weathered-bedrock zone, and by ~2–4 m depth, there is fresh, dense *mélange* with very low porosity that remains perennially saturated. Soil pits and hand augering revealed fine roots and fungal hyphae throughout the A and B horizons as well as the underlying weathered rock, to depths of at least 2 m. The A and B horizons are dilationally disturbed by roots and animal burrowing, leading to their progressive displacement downslope. Infiltrating rain collects in the pores of the weathered bedrock, and with sufficient rainfall, the pores become saturated throughout the subsurface, driving groundwater to the surface and promoting widespread saturation overland flow in the winter wet season (see descriptions in Hahm et al. 2017b and Lovill et al., *in press*).

Vegetation and study trees.—The site is characterized by heterogeneous vegetation communities. Areas underlain by predominantly *mélange* matrix are commonly grassland–savannah (on south-facing slopes) and woodland (on north-facing slopes). The herbaceous groundcover is primarily annual and non-native. *Quercus garryana* is the dominant woodland/savannah species, with occasional California buckeye (*Aesculus californica*) and California black oak (*Quercus kelloggii*). Recruitment patterns inferred from an exploratory tree survey in the study area of >2800 individual trees indicated that stand species composition does not appear to be changing (e.g., juvenile and seedling *Q. garryana* are the dominant under the canopy of mature *Q. garryana*, and typically not found elsewhere; Hahm et al. 2017c). Large sandstone blocks at the site support dense forests of Douglas fir and Pacific madrone (*Arbutus menziesii*). These vegetation assemblage patterns correlate with differences in seasonal water storage capacity controlled by the contrasting thickness and porosity of the subsurface weathered bedrock (Hahm et al. 2017b).

We chose small representative groups of monospecific stands of *Q. garryana* developed on the *mélange* for intensive study, and to account for possible effects of aspect, selected a stand from a savanna on a south-facing slope and from

woodland on the paired north-facing slope (Fig. 1). The trees ranged from 20 to 65 cm diameter at breast height (see Table 1). Canopy heights inferred from first vs. last return LIDAR (acquired by NCALM) and handheld impulse laser (Impulse 200 LR, Laser Technology, Englewood, Colorado, USA) ranged from 3.6 to 13.4 m. Mean canopy drip-line radii (calculated from the average of four cardinal directions) ranged from 3.0 to 7.4 m. Age determination from rings obtained via increment borers was not feasible due to the hardness of the heartwood; historical air photographs suggest that the study stands were established well before 1954, yielding a minimum age of 64 yr. The trees are situated on the sides of gently sloping hollows near channel heads (Fig. 1; Appendix S1: Fig. S1). The study trees, like most of the *Q. garryana* at the site, are variably colonized by evergreen American mistletoe (*Phoradendron leucarpum* subsp. *Tomentosum*).

Weather observations

In the spring of 2015, we installed a meteorological station in a grass-dominated area at the topographic divide between Hank and Dry creeks ~200 m east of the study trees (Fig. 1). The station records precipitation (Hyquest TB4), temperature and relative humidity (Vaisala HMP50-L, Vantaa, Finland), wind speed and direction (RM Young Wind Monitor 05103-L), total solar radiation (LiCor LI200X-L Pyranometer Shortwave), and barometric pressure (Vaisala PTB110, Vantaa, Finland) every 5 min. We calculated the vapor pressure deficit (VPD), defined as the saturated vapor pressure of the air (e_s) minus the actual vapor pressure of the air (e_a), from the relative humidity and the temperature following Snyder (2005).

Tree water potential measurements

Shoot water potentials (Ψ) were measured with a Scholander-type pressure chamber (Model 1000 Pressure Chamber Instrument, PMS Instrument Company; Albany, Oregon, USA), following procedures in Boyer (1995). We measured on a biweekly to monthly basis, from the end of the 2015 growing season to the end of the 2016 growing season. All shoots were collected between 1.5 and 2.5 m from the local ground surface. Immediately after excision, shoots were placed into sealed plastic bags in a dark container until measurement 5–60 min later. Pre-dawn Ψ samples

Table 1. Study tree characteristics.

Tree ID (tag #)	Slope aspect	Diameter at breast height (cm)	Average canopy radius (m)	Height (m; impulse laser-inferred)	Height (m; LIDAR-inferred)	UTM N (m)	UTM E (m)	Sapflow	Piston dendrometer	Pre-dawn & mid-day Ψ	Leaf K	Leaf pressure-volume curve
1	South	65.7	5.6	12.89	12.7	4,379,867.1	459,361.0	y	y	y	y	y
3	South	33.8	4.6	6.18	5.4	4,379,848.9	459,340.3	–	–	y	–	–
4	South	52.0	7.4	13.35	11.3	4,379,849.0	459,346.4	y	y	y	y	y
5	South	45.6	5.1	10.15	9.5	4,379,848.2	459,346.4	y	–	y	y	y
165	North	32.5	3.4	11.8	13.3	4,379,982.0	459,407.7	–	y	–	–	–
166	North	19.7	3.0	7.3	9.3	4,379,982.3	459,406.5	–	–	y	y	y
167	North	36.0	4.9	11.02	8.8	4,379,972.8	459,403.4	y	–	y	y	y
168	North	41.4	3.5	3.58	7.5	4,379,972.6	459,402.5	–	–	y	y	y

Notes: “y” indicates that the designated measurement was made or sensor was installed on this tree. The dash denotes lack of measurement or sensor.

were collected between 1.5 and 0.5 h before sunrise, and mid-day samples were collected between 11:00 and 14:30 hours, with two to three shoots collected from full to partial sun positions. We performed two averaging steps to report the pre-dawn and mid-day mean Ψ at a particular date, by first averaging all the shoots from an individual tree at a particular time of day, then averaging across all trees at the site. To highlight the seasonal evolution of the Ψ gradient from subsurface to shoot, indicative of stomatal control on mid-day Ψ and water acquisition strategy more generally, we also compare paired pre-dawn and mid-day Ψ for individual trees.

Interpretation of pressure chamber values.—Pre-dawn Ψ is considered diagnostic of subsurface water availability within the rhizosphere, subject to two factors that tend to bias this interpretation in opposite directions: (1) to the extent that sapflow continues at night, due to nighttime transpiration and/or tissue rehydration (Donovan et al. 2003, Dawson et al. 2007), the pre-dawn tree Ψ will remain lower than the rhizosphere Ψ , and (2) pre-dawn tree Ψ is biased toward the higher Ψ (wetter) reservoirs in the rhizosphere, due to higher hydraulic conductance in these areas (Améglio et al. 1999). Here, we adopt pre-dawn Ψ as the imperfect yet most physiologically relevant metric of subsurface water availability, and mid-day Ψ as the relevant metric impacting stomatal control and hydraulic limitations such as leaf turgor loss and hydraulic vulnerability of xylem.

Stem vs. leaf potential

In order to determine the magnitude of the Ψ drop between stem and leaf, we maintained

individual leaves in Ψ equilibrium with their stems at mid-day by preventing transpiration. To accomplish this, we bagged single leaves in plastic before sunrise to promote 100% relative humidity and enclosed them with foil to exclude sunlight. At mid-day, when the leaves received full to partial sunlight, we excised the bagged leaves and opposite non-bagged leaves from the same shoot at the base of the petiole with a razor blade and measured them in a pressure chamber. A variation of this method was employed by Hellkvist et al. (1974) to determine the gradient of Ψ along trunks, and earlier by Begg and Turner (1970), who referred to this method in analogy to a tensiometer placed into the tree.

Pressure–volume relations

Recent analyses suggest that relative symplastic water content (RWC_{sym}) and Ψ at the TLP (MPa, also known as the wilting point) are primarily functions of the osmotic potential at full turgor (Ψ_{S100} , MPa) and the symplastic cell wall modulus of elasticity (ϵ , MPa; Bartlett et al. 2012). These cell properties may adjust dynamically on both seasonal and diurnal timescales (Dawson and Bliss 1989, Meinzer et al. 2014) to depress the TLP and maintain hydraulic function at low Ψ . Leaves are typically fully rehydrated to an initial $\Psi = 0$ MPa prior to determination of pressure–volume (PV) curves; however, this rehydration may dynamically alter ϵ or Ψ_{S100} , and hence the inferred Ψ_{TLP} (see for example Meinzer et al. 1986). One approach to identifying this plasticity is to establish PV curves for both rehydrated and non-rehydrated leaves (to capture short-term dynamics), at different times throughout the course of the year (to capture

seasonal dynamics). We adopted this approach and collected shoots with 5–15 mature leaves at dusk or dawn, when water potentials were generally relaxed. To rehydrate samples, we excised leaves underwater near the petiole base with a razor blade and then left petioles in deionized water for >3 h in a dark cooler at $\approx 100\%$ relative humidity. We used a spreadsheet template designed by Cameron Williams (UC Berkeley/Franklin & Marshall College; see Williams et al. 2017) to visually identify and remove over-hydrated samples (the plateau effect) and determine all PV-curve parameters. Slopes and intercepts were determined via standardized major axis line fitting (Warton et al. 2006).

The principal metrics of interest were computed as follows: to estimate Ψ_{S100} , we plotted $-1/\Psi$ against $1 - \text{RWC}$ (total relative water content) and extrapolated the linear (post-TLP) part of the curve to the ordinate. RWC is a derived parameter that requires the leaf dry mass and saturated water content mass, obtained by extrapolation to the abscissa-intercept on a plot of Ψ vs. leaf water mass (this enables the estimation of saturated water content when the first water potential measurement is below zero or when the plateau/over-hydration effect is present; Kubiske and Abrams 1990). The apoplastic water fraction (AWF) is determined from the abscissa-intercept of $-1/\Psi$ vs. $1 - \text{RWC}$ post-turgor loss. We calculate ε (the symplastic cell wall modulus of elasticity) by finding the slope on a plot of the pressure component of cell water potential (Ψ_P) against RWC_{sym} prior to turgor loss. At turgor loss, Ψ_P goes to zero, and the osmotic potential (Ψ_S) fully defines the total water potential. Ψ_{TLP} can then readily be determined from the abscissa-intercept in a plot of pre-turgor loss Ψ_P vs. Ψ_S . We calculated absolute area-normalized leaf capacitance C ($\text{mmol}\cdot\text{m}^{-2}\cdot\text{MPa}^{-1}$) as the mass of water in a fully rehydrated leaf multiplied by the slope of RWC vs. Ψ and divided by A and the molecular weight of water (Blackman and Brodribb 2011).

Leaf hydraulic conductance

We estimated leaf hydraulic conductance (K) as a function of leaf Ψ using the leaf-as-a-capacitor method (Brodribb and Holbrook 2003). On 26 July 2016, between 06:00 and 06:30 hours, we collected branches with multiple shoots from six *Q. garryana* individuals (the same individuals

instrumented with sapflow sensors and seasonally monitored for Ψ). Pressure–volume relations from leaves from these branches were determined, including pre-turgor loss C . The branches were recut under water and left to rehydrate with their cut ends in water in a dark cooler. On 27 July 2016, we removed the cut ends from water and allowed the branches to slowly dry on the laboratory bench. Prior to determining leaf Ψ , we sealed branches in dark coolers for at least 20 min to promote equilibration of water potential among leaves. We selected one leaf, measured its initial Ψ_0 with a pressure chamber, then cut its closest neighbor underwater, and allowed it to rehydrate through the petiole for 15–40 s. We then immediately determined the final Ψ_f . We calculate leaf K ($\text{mmol}\cdot\text{m}^{-2}\cdot\text{s}^{-1}\cdot\text{MPa}^{-1}$) via $K = C \ln [\Psi_0/\Psi_f]/t$, where t is time in seconds (Brodribb and Holbrook 2003). We used the pre-turgor loss C ($255 \text{ mmol}\cdot\text{m}^{-2}\cdot\text{MPa}^{-1}$) from rehydrated leaves for all measurements, even when the initial water potential was below the mean TLP of leaves collected that day. We opt for this method because most Ψ_0 and Ψ_f points were above or spanned the TLP.

Sapflow

We measured trunk sapflow every half hour from midsummer 2015 to fall 2016 on four trees (Table 1) with copper–constantan thermocouples at 12.5 mm depth into the sapwood (ICT International Pty, sensor model HRM30, Armidale, Australia; see Marshall 1958). All sensors were placed between 2.5 and 3.5 m above the ground along the main trunk below any photosynthetic tissue and secondary branches, in order to minimize interference from cattle, deer, elk, and black bear. Because probes are rarely perfectly spaced, at times of no flow a non-zero velocity may be inferred. To correct for this, following Link et al. (2014), we assume that no gradient in water potential to leaves is maintained during the three hours before sunrise when relative humidity is between 92% and 95%. At lower humidity, nighttime sapflow may occur due to non-negligible VPDs; at higher humidity, dew may condense on leaves, resulting in rehydration and sapflow toward roots. At these times, we take the median sapflow velocity for each sensor to be the true zero flow rate. We then employed the correction procedure for the heat-ratio method outlined in

Burgess et al. (2001) to rescale all datapoints to the zero flow rate, assuming a thermal diffusivity of $2.5 \times 10^{-3} \text{ cm}^2/\text{s}$. To compare trends in the seasonal and diurnal patterns in sapflow between trees in relation to subsurface water availability and leaf water potential, we normalized all sapflow velocities, following Link et al. (2014). First, we identified outliers clearly attributable to sensor malfunction, which led us to trim the dataset to exclude values below -5 and above 50 cm/h . Occasional unphysical spikes or drops in sapflow were still present in the resulting datastream, which we eliminated by trimming the dataset again to exclude values below the 2.5 and above the 97.5 percentiles recorded for the entire time series of each individual sensor. We normalized the resulting dataset to the maximum value recorded by each individual sensor during its deployment. We present the entire datastream from each sensor, with a slight transparency to display the changing relative density of data. This time series highlights the daily maxima and minima sapflow throughout the measurement campaign in relation to environmental variables. We also determined the seasonality of total sapflow for each tree by summing normalized sapflow velocities by month, then averaging the resulting sums across all trees. When half-hourly data were missing due to equipment malfunction, we used linear interpolation to infill. We also sought to analyze seasonal changes in the diurnal sapflow pattern by averaging the normalized daily sapflow pattern by month, then averaging across all trees.

Piston dendrometers

To measure seasonal growth patterns and diurnal patterns of water storage, we installed point piston dendrometers (Natkon Model ZN11-T-WP, resolution of $\approx 1 \mu\text{m}$; see Zweifel et al. 2006) on trunks, adjacent to the sapflow probes. The dendrometers measured the combined radial displacement of inner bark, cambium, and sapwood relative to a heartwood frame of reference. Sapwood is the largest component volumetrically, typically composing 15% of stem basal area in *Q. garryana* (Meinzer et al. 2005). We used a rolling median filter with a single timestep limit of $10 \mu\text{m}$ to filter occasional sensor noise. We show the time series during the 2016 growing season of the three trees that did

not experience sensor malfunction (#165, 1, and 4), and the average composite diurnal pattern by month of these same trees to highlight the daily patterns of growth and the magnitude of water storage and extraction.

RESULTS

All terms, symbols, and units are defined in Table 2.

Weather

The rain gauge recorded 1976 mm of precipitation in the 2016 water year (Fig. 2). This relatively wet winter was preceded by four years of drought that affected most of the state of California. No crown dieback was observed on any of the trees selected for this study at the end of the drought or in 2016 following the wetter winter, nor for that matter on any of the mature *Q. garryana* at the site. The last major winter storms of 2016 occurred in April, totaling 76 mm of precipitation, followed by minor storms in May (20 mm) and June (17 mm), with no measured precipitation in July, August, or September. Maximum daily summer temperatures routinely exceeded 30°C , and during heat waves, nighttime minima did not fall below 20°C . These high

Table 2. Symbols, units, and terms.

Symbol	Units	Term
K	$\text{mmol}\cdot\text{m}^{-2}\cdot\text{MPa}^{-1}\cdot\text{s}^{-1}$	Leaf hydraulic conductance
C	$\text{mmol}\cdot\text{m}^{-2}\cdot\text{MPa}^{-1}$	Leaf hydraulic capacitance
TLP	MPa	Turgor loss point
Ψ	MPa	Water potential
Ψ_s	MPa	Osmotic potential
Ψ_{s100}	MPa	Osmotic potential at full turgor
Ψ_p	MPa	Pressure potential
ϵ	MPa	Symplastic cell wall modulus of elasticity
$\text{RWC}_{\text{total}}$	(decimal)	Total leaf relative water content
RWC_{sym}	(decimal)	Leaf symplastic relative water content
AWF	(decimal)	Apoplastic water fraction
A	cm^2	One-sided leaf area
SLA	m^2/kg	Specific leaf one-sided area
LMA	g/m^2	Leaf mass per one-sided area

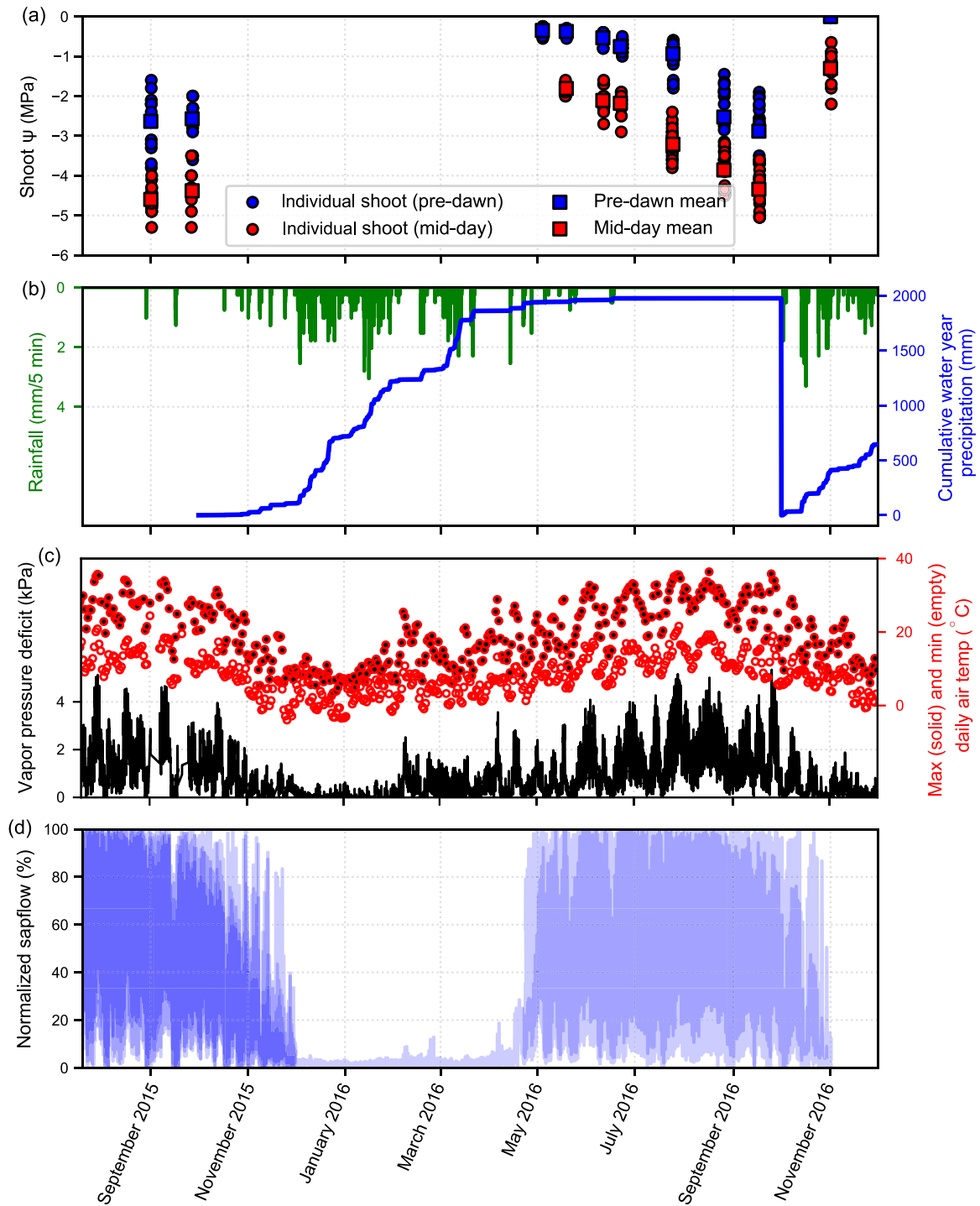


Fig. 2. Time series of (a) pre-dawn and mid-day shoot Ψ , (b, c) climate, and (d) sapflow in mature *Quercus garryana*. Sapflow remains high in late summer (d) in spite of low subsurface water availability (low pre-dawn Ψ in a), and lack of summer precipitation (b). In (d), slight transparencies highlight the density of data. Cumulative water year precipitation in (b) is missing for 2015 due to incomplete record. Non-zero sapflow during winter when *Q. garryana* lacks leaves in (d) is attributable to evergreen mistletoe.

temperatures resulted in daytime VPDs above 4 kPa, and on warm nights, the VPD remained above 1 kPa.

Leaf phenology

Leaves on *Q. garryana* at Sagehorn emerge rapidly in late April through mid-May, and persist until mid- to late November, longer than co-occurring *Q. kelloggii*. *Quercus garryana* on south-facing slopes tend to keep their leaves 1–2 weeks longer than those inhabiting north-facing slopes. We did not observe drought-deciduous behavior in four years of observation (2014–2017); instead, most leaves typically fall after the first significant wet-season rains.

Tree water potential

Seasonal pattern.—Pre-dawn shoot Ψ declined throughout the 2016 growing season (Fig. 2), from mid-May pre-dawn values of -0.38 ± 0.02 MPa, $n = 7$ (mean of individual tree mean \pm individual tree means standard error, $n =$ number of trees) and -1.81 ± 0.03 MPa, $n = 7$ (at mid-day) to mid-September pre-dawn values of -2.88 ± 0.34 MPa, $n = 6$, and mid-day values of -4.34 ± 0.22 MPa, $n = 6$. Two trees (#4 and #166) had average pre-dawn Ψ below -3.5 MPa by mid-September. With the return of fall rains in early November, pre-dawn Ψ rose to values indistinguishable from 0 MPa. Both intra-tree and inter-tree Ψ heterogeneity increased as the growing season progressed, with pre-dawn and mid-day values tightly clustered in May and exhibiting large scatter by September.

Time course of hydraulic gradient.—Fig. 3 shows pre-dawn vs. mid-day shoot Ψ paired by individual tree on a particular sample day throughout the growing season. On average, a 1.6 MPa hydraulic gradient is maintained in spite of absolute declines in potential: The gradient at the start of the dry season, when pre-dawn Ψ was on average -0.4 MPa, was not markedly different than at the end of the dry season, when pre-dawn Ψ in some trees approached -4.0 MPa.

Stem, leaf, and shoot Ψ .—Fig. 4 shows a sharp drop (~ 1.2 MPa) between leaf and stem Ψ at mid-day. Mid-day shoot Ψ lies between leaf and stem Ψ , and is closer to leaf Ψ than stem Ψ (Table 3),

consistent with shoot Ψ representing a weighted average of leaf and stem. In late summer (26 August 2016), the Ψ drop between mid-day stem and mid-day leaf was larger than the Ψ drop between pre-dawn shoot and mid-day stem.

Leaf water relations inferred from pressure–volume curves

The pressure–volume curves exhibited high coefficients of determination ($R^2 > 0.95$) for linear relationships between pre-turgor loss Ψ_P vs. Ψ_S and post-turgor loss $1/\Psi$ vs. $1 - \text{RWC}$ (see example relations and graphical definitions of terms from one individual leaf in Appendix S1: Fig. S2; parameters for all leaves are summarized in Table 4). Curves with fewer than four pre-turgor loss measurement points were discarded. This resulted in the loss of three non-rehydrated leaves from the 17 September 2016 measurement campaign, which we infer were too close to the TLP at the start of measurement. The average TLP for all measurements was -3.61 MPa (Table 4) and varied by nearly 1 MPa across initial hydration status and dates, from a high of -3.28 MPa for rehydrated leaves on 26 July 2016 to a low of -4.26 MPa for non-rehydrated leaves on 17 September 2016. The TLP increased when leaves were rehydrated and generally decreased

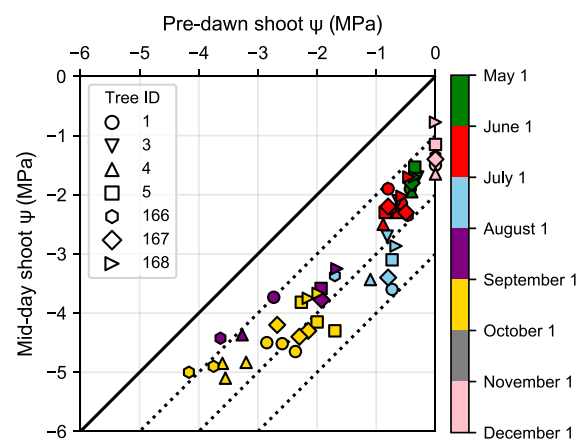


Fig. 3. Pre-dawn vs. mid-day shoot Ψ of individual mature *Quercus garryana*, color-coded by measurement month in the 2015 and 2016 growing seasons. November measurements taken after return of wet-season rains in 2016. The diagonal dashed lines show -1 , -2 , and -3 MPa isopotential gradients for reference.

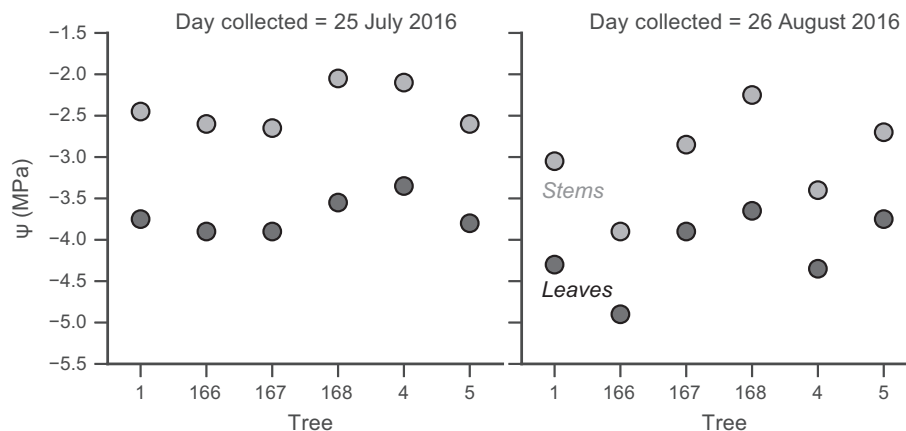


Fig. 4. Comparison of stem and leaf Ψ from the same shoot at mid-day across two summer days shows consistent >1 MPa hydraulic gradient from stem to leaf. Numbers on horizontal axis refer to tree ID (see Table 1 and site map in Fig. 1).

throughout the season. The average Ψ_{S100} for all measurements was -2.93 MPa, and Ψ_{S100} varied by a relatively smaller extent between initial hydration status and dates, from an average high of -2.74 MPa for rehydrated leaves to an average low of -3.17 MPa for non-rehydrated leaves. Ψ_{S100} decreased slightly on average throughout the season and tended to decrease with rehydration. Bulk tissue elastic modulus, ϵ varied little seasonally, but showed a strongest response to rehydration, approximately doubling on each date from values of ≈ 10 to ≈ 20 MPa, translating to much more rigid leaf tissue at higher initial water contents. RWC_{sym} at the TLP also varied systematically with initial hydration status but not season, with rehydrated leaves exhibiting much higher RWC_{sym} than non-rehydrated leaves. The size of leaves measured for PV curves did not vary systematically.

Leaf hydraulic conductance (K)

K decreased with decreasing leaf Ψ in a sigmoidal fashion (Fig. 5). A Weibull-type vulnerability curve fit to the data indicates that the maximum K is $13.7 \text{ mmol}\cdot\text{m}^{-2}\cdot\text{MPa}^{-1}\cdot\text{s}^{-1}$. The midpoint (50% loss between maximum and minimum) occurs at a leaf Ψ of -3.35 MPa, and $>95\%$ of the loss occurred over a range of 2 MPa spanning this midpoint. K inferred at low Ψ would be approximately two times lower than presented values if the post-TLP capacitance was used in calculations.

Sapflow

Diurnal trends.—Sapflow exhibits a common diurnal pattern throughout the primary growing season (May–September; Fig. 6 shows composite monthly averaged patterns across all trees). At pre-dawn sap flows in the trunk, from an April average of $\sim 5\%$ of the maximum, increasing to 12% during the driest, hottest month of the year. Sapflow increases rapidly and monotonically for four hours after sunrise, on average across all trees studied $\sim 60\%$ of the total range. A mid-day depression occurs, after which sapflow rebounds to a daily peak in the mid-afternoon in the summer months between 70% and 90% of the maximum recorded sensor value. With decreasing sunlight, sapflow declines at a lower rate than the morning rise for five to six hours and at sunset is typically $\approx 25\%$ of the maximum value (a factor of ≈ 2 higher than the pre-dawn value).

Table 3. Comparison of Ψ along the subsurface–plant–atmosphere continuum on two dry-growing season days.

Parameter	Ψ (–MPa, average \pm standard error of the mean)	
	25 July 2016	26 August 2016
Pre-dawn shoot	0.94 ± 0.14 ($n = 20$)	2.53 ± 0.33 ($n = 17$)
Mid-day stem	2.38 ± 0.10 ($n = 6$)	3.03 ± 0.23 ($n = 6$)
Mid-day shoot	3.21 ± 0.12 ($n = 21$)	3.86 ± 0.19 ($n = 15$)
Mid-day leaf	3.66 ± 0.09 ($n = 6$)	4.14 ± 0.19 ($n = 6$)

Note: n refers to total number of samples measured across multiple individual trees.

Table 4. Leaf metrics derived from pressure–volume (PV) curve experiments on mature *Quercus garryana* individuals, across sampling days and hydration status.

Day and hydration status	<i>n</i>	Dry mass (g)	<i>A</i> (cm ²)	SLA (m ² /kg)	LMA (g/m ²)	TLP (MPa)	Ψ _{S100} (MPa)	ε (MPa)	AWF	RWC _{sym} @TLP
22 June 2016										
Rehydrated	7	0.45 ± 0.15	43.3 ± 18.9	9.40 ± 1.97	110.1 ± 21.1	-3.44 ± 0.32	-2.94 ± 0.35	20.0 ± 5.6	0.20 ± 0.16	0.85 ± 0.03
26 July 2016										
Non-rehydrated	5	0.40 ± 0.08	33.4 ± 9.3	8.30 ± 1.38	123.0 ± 18.3	-3.67 ± 0.44	-2.74 ± 0.21	10.5 ± 1.7	0.18 ± 0.04	0.75 ± 0.04
Rehydrated	5	0.36 ± 0.14	32.0 ± 9.1	9.38 ± 1.64	109.4 ± 19.8	-3.28 ± 0.52	-2.84 ± 0.46	21.6 ± 6.7	0.08 ± 0.24	0.86 ± 0.03
17 September 2016										
Non-rehydrated	2	0.42 ± 0.07	35.0 ± 5.7	8.25 ± 0.03	121.2 ± 0.4	-4.26 ± 0.25	-3.06 ± 0.52	10.4 ± 5.8	0.07 ± 0.03	0.72 ± 0.08
Rehydrated	5	0.45 ± 0.13	35.8 ± 10.5	7.95 ± 0.85	126.9 ± 13.8	-3.85 ± 0.23	-3.17 ± 0.10	17.9 ± 2.4	0.20 ± 0.02	0.82 ± 0.03
All leaves	24	0.42 ± 0.12	36.6 ± 12.8	8.77 ± 1.54	117.1 ± 18.2	-3.61 ± 0.45	-2.93 ± 0.34	17.1 ± 6.3	0.16 ± 0.14	0.81 ± 0.06

Notes: Mean ± 1 standard deviation. See Table 2 for abbreviations.

A slow monotonic decline continues until dawn. In April and October, which bookend the growing season, sapflow does not rise to midsummer highs. Nighttime flows are similarly reduced but remain positive pre-dawn.

Seasonal trends.—Phenological observations of leaf out and leaf loss indicate that the early-season (April–May) ramp-up of sapflow coincided with increasing leaf area, and late-season (October–November) declines in sapflow coincided with leaf loss. During the months of highest photosynthetically active radiation, from the beginning of May through mid-September, sapflow returned to near its maximum recorded value for each tree each day but declined in response to short-duration (1–3 d) storms (Fig. 2). Total sapflow (which is directly correlated with total transpiration) reached a peak in midsummer (Fig. 7), when atmospheric moisture demand was highest and subsurface water availability was low, as indicated in the VPD and pre-dawn Ψ time series (Fig. 2). High sapflow throughout the dry-growing season occurred while shoots maintained hydraulic gradients with the subsurface of >1 MPa (Ψ difference between pre-dawn and mid-day), even as both pre-dawn and mid-day water potentials declined (Fig. 3). In the winter wet season, sapflow continued on leafless trees parasitized with evergreen mistletoe on warm, dry days (Fig. 2), indicating that some portion of the hydraulic pathway remained active throughout the year. We do not know the extent to which mistletoe accounts for total sapflow in summer, although

its relatively small leaf area suggests its contribution should be minimal.

Piston dendrometers

Seasonal trends.—The sapwood, cambium, and inner bark increased in size radially in the early part of the growing season (April–July) by ≈1–3 mm, then remained approximately constant in size during the latter half of the summer (July–September; Fig. 8). Rain in April and May as well as October abruptly increased radial size, which then shrunk slowly over the course of a few days.

Diurnal trends.—Each day, the sapwood, cambium, and inner bark increase in size until early

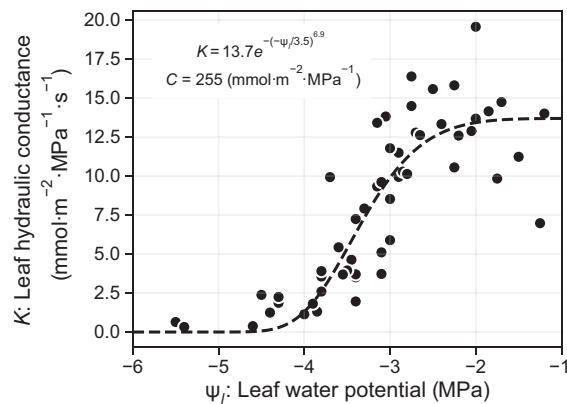


Fig. 5. Leaf hydraulic vulnerability curve shows decline in the leaf hydraulic conductance (*K*) as leaf water potential (Ψ) declines.

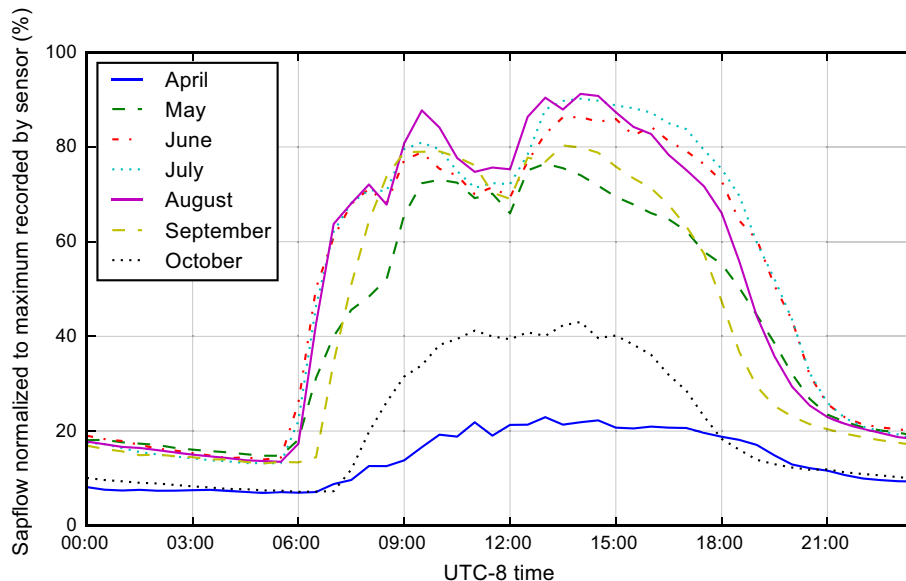


Fig. 6. Average diurnal sapflow pattern across each month of the 2016 growing season. Sapflow is high in the dry-season summer months, continues at night, and exhibits a mid-day depression. Closer to the solstice, the onset of sapflow in the morning occurs earlier and the evening decline occurs later. Curves do not reach 0% or 100% as the monthly averaged behavior shown here averages across multiple trees and includes days when sapflow did not reach the minimum or maximum recorded.

dawn, then begin to shrink as the sun rises, until late afternoon when they begin to increase again through the night (Fig. 9). Net positive radial size increases of $\approx 20 \mu\text{m/d}$ occur in the early (April–June) and late (October) months of the growing season, consistent with the seasonal observations of net positive displacement in Fig. 8. The daily amplitude of radial size change increases from $\approx 10 \mu\text{m}$ in the early spring to $\approx 25 \mu\text{m}$ in the late summer months. The dendrometers recorded continual size changes, with no month exhibiting a time of day when radial size remained constant.

DISCUSSION

Here, we discuss the interacting environmental and physiological factors that regulate *Quercus garryana*'s water relations. We contrast our findings with previously published reports on a variety of oaks and *Q. garryana*'s perceived competitor, *Pseudotsuga menziesii*. We then step back and juxtapose these individual observations with the effects of modern and paleoclimate shifts on these species' populations.

Together, the data lead us to conclude that *Q. garryana* is an exceptionally water-limitation-tolerant species that will be favored in the presently warming climate.

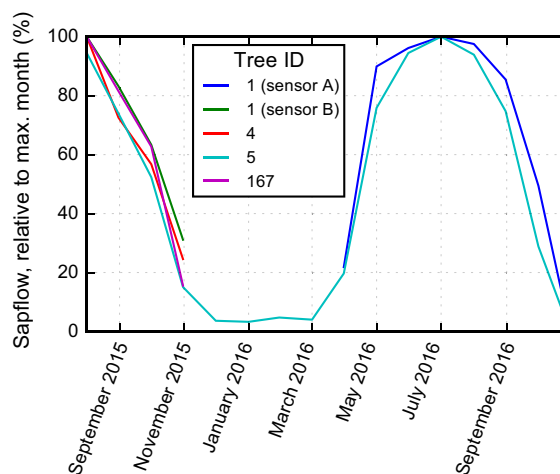


Fig. 7. Total integrated sapflow per month, normalized to the maximum month recorded by each sensor. Sapflow peaks during the summer months with greatest insolation in spite of negligible precipitation.

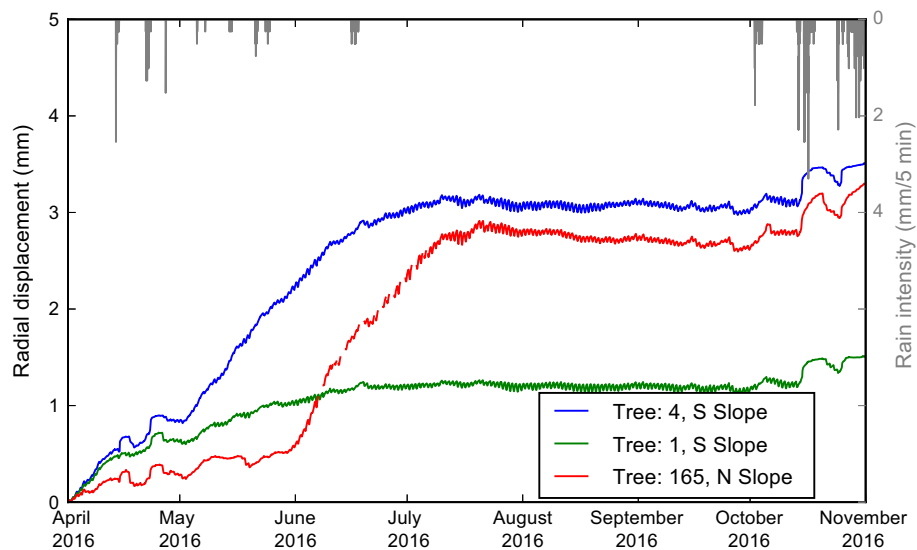


Fig. 8. Radial displacement of sapwood, cambium, and inner bark away from the trunk in the 2016 growing season. Early growing season increase reflects sapwood growth. Smaller amplitude oscillations (see Fig. 9) reflect diurnal water storage and release. Abrupt increases that decay after a period of days reflect rehydration of inner bark and sapwood due to rain (vertical gray lines, right y -axis).

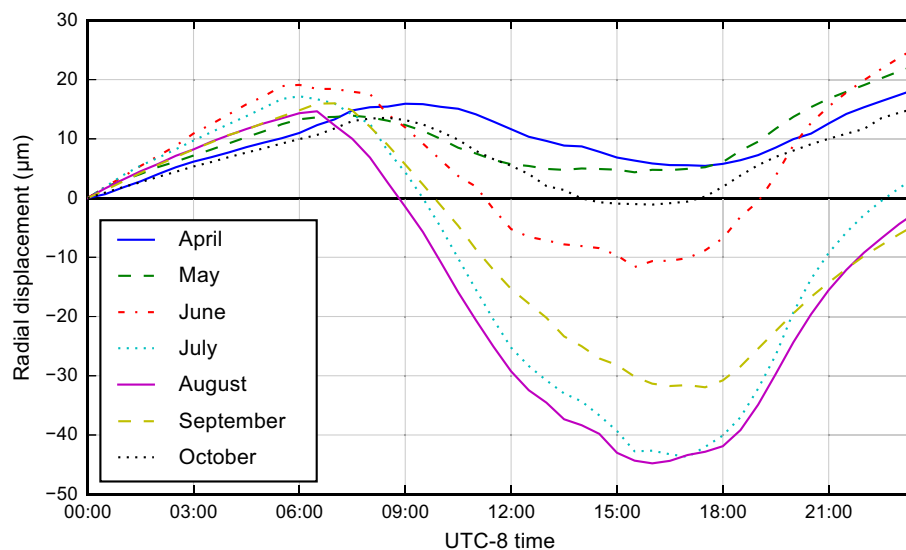


Fig. 9. Average daily displacement of sapwood, cambium, and inner bark away from the trunk in a heartwood reference frame (positive is radially outward) across all instrumented trees each month of the 2016 growing season. The start of each 24-h period is fixed to zero to highlight inter-month dynamics. Spring–early summer months exhibit net positive daily displacement, reflecting sapwood growth, and the amplitude of displacement is highest in midsummer, reflecting greatest daily uptake and release of stored water.

Water potential

Relatively high and uniform pre-dawn Ψ in May likely reflect access to shallow groundwater. Pre-dawn Ψ slowly declined for three months from the beginning of May and remained above -1 MPa in late July on average (Fig. 2). One month later, pre-dawn values were below -2.5 MPa. This precipitous drop is likely caused both by the declining availability of easily extracted groundwater (see also Hahm et al. 2017a) and an inflection point in the subsurface water characteristic curve, where at low volumetric water contents water potential may decrease rapidly during drying (we lack characteristic curve measurements to confirm this). Sitewide average late-season (mid-September) 2016 Ψ values were similar to late-season (late September) 2015 Ψ values of -2.57 ± 0.28 MPa, $n = 5$ (pre-dawn; mean \pm standard error of the mean, number of trees), and -4.38 ± 0.22 MPa, $n = 5$ (mid-day), consistent with a common seasonal evolution of pre-dawn Ψ across years, in spite of confounding factors such as varied late spring rains, one week difference in sampling dates, and different total water year rains. This common evolution of Ψ may arise due to an upper limit on subsurface water storage at the site that is much less than mean annual precipitation, as explored in Hahm et al. (2017b).

The pre-dawn Ψ observed here is far lower than previous reports of mature *Q. garryana*. Late summer *Q. garryana* pre-dawn Ψ across a wide range of sites in Oregon was > -1.5 MPa on average in 60-yr-old, 13 m tall individuals (Kelly 2016), ≈ -0.5 MPa in mid-late summer for ≈ 15 -yr-old individuals (Johnson et al. 2009), > -1.5 MPa for stump sprouts to 30-yr-old individuals (Davis 2005), and > -1.0 MPa for 30 m tall individuals (Phillips et al. 2003a). The Ψ we observed is higher, however, than the pre-dawn summer Ψ in mature *Q. douglasii* of ≈ -6.2 MPa in the foothills of the Sierra Nevada (Xu and Baldocchi 2003). Anderson and Pasquinelli (1984) found *Q. douglasii* replacing *Q. garryana* along a mesic-to-xeric moisture gradient in Sonoma County, and the *Q. douglasii* range generally extends into more xeric habitat, indicating that it is likely more water-limitation tolerant.

Seasonally declining mid-day Ψ to maintain sapflow indicates that in this particular environment stomata remain open, enabling carbon assimilation in desiccating conditions. This is

consistent with the observation of greenhouse-grown *Q. garryana* seedlings maintaining positive carbon assimilation rates even after a 42-d period of drying when soil volumetric water content dropped below 2% (Merz et al. 2017). Davis (2005) similarly plotted mid-day vs. pre-dawn Ψ of mature *Q. garryana* in Oregon (Davis 2005: Figure 3.10) and found a steep slope across the range of pre-dawn Ψ observed (to approximately -1.5 MPa).

Meinzer et al. (2016) observed the Ψ evolution of *Q. garryana* seedlings subjected to drought in a greenhouse and also found large pre-dawn to mid-day $\Delta\Psi$ (>1 MPa) at pre-dawn water potentials < -4 MPa. However, as their drought experiment continued, pre-dawn Ψ equaled mid-day Ψ at -6 MPa, indicating that there was no longer a gradient between root and shoot, consistent with stomatal closure (or hydraulic failure). This suggests that strict anisohydric behavior (sensu McDowell et al. 2008) does not apply to *Q. garryana*'s water-use regulation across the entire range of extreme dry conditions that may be encountered in nature, consistent with recent work that suggests that where plants map onto the anisohydric–isohydric continuum is likely contingent on intrinsic factors as well as the environmental conditions experienced (Meinzer et al. 2016, Martínez-Vilalta and Garcia-Forner 2017).

Stem, leaf, and shoot Ψ .—The Ψ drop between root and stem, which occurs over a relatively long distance (order decameter), is of the same order of magnitude as that between stem and leaf (order decimeter; Table 3). Continuity of sapflow implies a large increase in resistance in the hydraulic pathway at the stem–leaf transition, due to either lower hydraulic conductivity or smaller functional xylem cross-sectional area, which reduce the hydraulic conductance (K). This indicates a much lower K in the leaf than in the roots, trunk, and distal stems. The leaf vulnerability curve is consistent with this finding: Leaf K drops dramatically at low leaf Ψ (Fig. 5). Stem hydraulic conductivities measured elsewhere in *Q. garryana* indicate that they may decline less in response to declining Ψ . Davis (2005) found relatively high rates of leaf-specific twig xylem hydraulic conductivity that did not change significantly throughout the growing season. Domec et al. (2007) found relatively high rates of trunk-specific conductivity, and Merz et al. (2017) observed that stem hydraulic

conductivity losses remained below 50% to < -3.6 MPa in seedlings.

Leaf pressure–volume curves

Comparison of leaf parameters and dynamic adjustment.—The TLP (-3.61 MPa) and Ψ_{S100} (osmotic potential at full turgor; -2.93 MPa) measured in this study for *Q. garryana* are both below 95% of reported values in a global compilation of 248 (TLP) and 303 (Ψ_{S100}) species, spanning a broad range of climatic settings (Bartlett et al. 2012). This is a first-order indication of the ability of *Q. garryana*'s leaves to maintain basic hydraulic function at the low water potentials encountered in the course of a dry season or drought. Three previous studies report TLP values for *Q. garryana* of ≈ -3.45 MPa (seedlings; Meinzer et al. 2016), ≈ -3.95 MPa (Johnson et al. 2009) and -3.2 to -3.6 MPa (Davis 2005). These values were all derived from rehydrated leaves from Oregon and fall within the range of values we measured for individual leaves, indicative of a general convergence in this trait across its geographic range.

Davis (2005) also reported Ψ_{S100} which was higher (between -2.00 and -2.75 MPa) than found in this study, suggesting that an environmental or genetic factor affects this leaf property. The comparable TLP of Davis (2005) in spite of higher Ψ_{S100} may be attributable to generally low ϵ (elasticity; ≈ 13.5 MPa). This is because a decrease in either Ψ_{S100} or ϵ lowers the TLP, as described by Bartlett et al. (2012): $TLP = (\epsilon \Psi_{S100}) / (\epsilon + \Psi_{S100})$ (depicted graphically by the contour plot in Fig. 10). Bartlett et al. (2012) found that the TLP is more sensitive to changes in Ψ_{S100} than ϵ given the range of common plant values; that is, a 1 MPa decrease in Ψ_{S100} will typically depress the TLP much more than a 1 MPa decrease in ϵ . Furthermore, in a global meta-analysis of biomes associated with different water supplies, Bartlett et al. (2012) found that adjustments in Ψ_{S100} , and not ϵ , primarily explained adjustments in the TLP that conferred water-limitation tolerance to dry-biome species. The analytical expression of TLP from Bartlett et al. (2012) predicted the TLP we derived (see Appendix S1: Fig. S2), except at very low TLP (Fig. 10 inset plot). Furthermore, an equivalent change in Ψ_{S100} has a much larger effect on TLP

than ϵ across most of the leaves studied here. However, because ϵ varied much more ($\sim 100\%$ relative change) than Ψ_{S100} ($\sim 15\%$ relative change) across sample dates and initial hydration status, the *Q. garryana* TLP was also sensitive to ϵ , particularly as it approached values < 10 MPa (Fig. 10). This effect was most pronounced between non-rehydrated and rehydrated leaves, with rehydrated leaves exhibiting a stiffening of the cell wall (increasing ϵ) and consequently a diminishing effect on TLP.

Sustained sapflow and stomatal opening at Ψ below the TLP.—We observed high sapflow in late summer (Fig. 7) as pre-dawn shoot Ψ dropped below -3.6 MPa and mid-day shoot Ψ dropped below -4.5 MPa (Fig. 3). Leaves experienced even lower Ψ (Table 3). Given the average TLP of -3.61 MPa, this indicates that stomata remained open during leaf turgor loss. Johnson et al. (2009) observed maximum daily stomatal conductance in *Q. garryana* coincident with daily minimum leaf Ψ at -3.6 MPa. Mitchell et al. (2008) observed pre-dawn leaf Ψ lower than the TLP inferred from PV curves of rehydrated leaves for species growing in a dry biome in

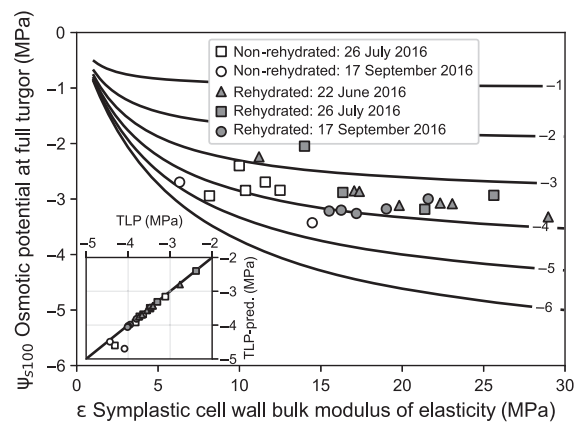


Fig. 10. The turgor loss point (TLP; labeled contours) as a function of Ψ_{S100} and ϵ , based on the analytical formulation of Bartlett et al. (2012). The TLP is more sensitive to Ψ_{S100} than ϵ for a given 1 MPa change in either term, but ϵ varies much more than Ψ_{S100} , and is lower for non-rehydrated leaves, illustrating a potential mechanism for TLP depression in leaves experiencing low Ψ . Inset shows TLP (x-axis) inferred as described in *Methods* section and illustrated in Appendix S1: Fig. S2 compared to analytical prediction of Bartlett et al. (2012) as a function of Ψ_{S100} and ϵ .

southwest Australia, and Meinzer et al. (2016) documented *Q. garryana* seedlings with pre-dawn $\Psi < -4$ MPa and mid-day Ψ nearing -6 MPa (Meinzer et al. 2016: Figure S4), with a TLP of ≈ -3.45 MPa (Meinzer et al. 2016: Figure 4). Farrell et al. (2017) concluded that water-limitation-tolerant plants can keep stomata open at Ψ lower than the TLP. Continued sapflow at Ψ lower than the TLP suggests that (1) leaf stomata remain open and sapflow continues post-turgor loss, (2) dynamic depression of the TLP occurs, and that this depression is poorly captured in traditional PV curves, (3) the TLP occurs at different Ψ for different cells in the leaf, with the PV curve inferred bulk leaf average TLP possibly higher than guard cell TLP, or (4) leaf Ψ lowers substantially between excision and measurement in the pressure chamber. While condition (4) must occur to some extent in *Q. garryana*, it seems unlikely to produce the large (>1 MPa) discrepancies noted above, especially at pre-dawn when stomata are shut and given the observation in obtaining PV curves that uncovered leaves lose water slowly at low Ψ . The most likely explanation for continued sapflow at pre-dawn Ψ below the TLP is a poorly captured dynamic adjustment of TLP in traditional PV curves. This explanation is also consistent with visual assessment of leaves in the field that remain healthy and turgid (Appendix S1: Fig. S3). Large changes occurred in important leaf metrics like RWC_{sym} @ TLP and ε between rehydrated and non-rehydrated leaves, suggesting that further, difficult-to-detect changes may occur as leaves near the TLP.

Leaf hydraulic conductance (K)

Reductions in K with declining leaf Ψ like those in Fig. 5 are common in many species, but the precise mechanisms of K loss and recovery and the consequences for sapflow remain poorly understood. Johnson et al. (2009), employing the same method as this study, showed that K in leaves of *Q. garryana* from Oregon declined in a similar pattern with decreasing Ψ , with a slightly lower Ψ at 50% loss of K (-3.61 MPa [Johnson et al. 2009] vs. -3.35 MPa [this study]). We observed high rates of sapflow at the end of the dry season coincident with mid-day Ψ that would have resulted in significantly reduced leaf K . A large drop in Ψ occurs between the stem

and leaf (Table 3), so that declining K may not inhibit leaf function due to the compensatory effect of a larger Ψ gradient across the leaf.

Sapflow dynamics

The *Q. garryana* studied here maintained high rates of sapflow even as pre-dawn Ψ dipped below -3 MPa and VPDs exceeded 4 kPa. This indicates that *Q. garryana* is water-limitation tolerant, leaving stomata open during the dry Mediterranean summer that coincides with high incoming photosynthetically active radiation, thereby promoting carbon acquisition. This behavior contrasts with the seasonal timing of transpiration of the codominant plant functional group at the site (annual grasses), which transpire the most in the wet spring and lose their green photosynthetic tissue by midsummer.

Fisher et al. (2007) observed high rates of sapflow during the summer in *Q. douglasii* (which is genetically similar to *Q. garryana*), with integrated sapflow similar to the seasonal cycle we observed (Fig. 7). Fisher et al. (2007) also observed nighttime sapflow which they attributed to transpiration. That nighttime sapflow was strongly correlated with VPD, consistent with the observations in this study. Pre-dawn sapflow can remain at $>20\%$ of the maximum on nights when VPD remains high (Fig. 2). The only other studies to our knowledge presenting time series of sapflow data in mature *Q. garryana* (Phillips et al. 2003a, b) showed similar daytime patterns and also found relatively minor differences in total daily water flux between early and late season in spite of declining pre-dawn Ψ . Phillips et al. (2003a, b) found that sapflow in *Q. garryana* approached zero pre-dawn, unlike the trees in this study.

Quercus spp. on the East coast of the United States in the Shale Hills CZO displayed remarkably different responses to declining soil moisture and increases in VPD: In the summer, after a rain event, sapflow declined by 62% in *Quercus alba*, *Quercus prinus*, *Quercus rubra*, and *Quercus velutina* over a period of just five days (Gaines et al. 2016). This is consistent with a heightened sensitivity to moisture declines in the very near surface: Rooting density was observed to be concentrated across all topographic positions within 50 cm of the surface, and the trees showed strong isotopic evaporative enrichment signals

consistent with sourcing water from shallow, rapidly drying soils. In contrast, Devine and Harrington (2005) noted that half of the cross-sectional area of first-order lateral roots branching from the taproot of *Q. garryana* growing in a glacial outwash soil was found below 30 cm, and mats of fine roots were found in moist lenses below 150 cm. Ugolini and Schlichte (1973) found that *Q. garryana* commonly has deep taproots extending below the surface soil. These observations of deeper, subsoil rooting are also common in *Q. agrifolia* and *Q. douglasii* in California (Cannon 1914, Lewis and Burgy 1964, Griffin 1973, Miller et al. 2010). This highlights a greater reliance of eastern oak species on frequent summer storms for delivery of water to surface soils, in contrast to the western oaks that are better adapted to the dry-growing season of Mediterranean climates.

Growth and water storage dynamics inferred from piston dendrometers

The radial changes in Figs. 8 and 9 reflect seasonal growth and tissue water storage and release. Most of the radial increase occurs in the early part of the growing season, which we attribute to sapwood growth, consistent with observations elsewhere that *Q. garryana* rings show a continuously declining amount of latewood relative to earlywood as the tree grows (Lei et al. 1996), and dendrometer-band inferred diameter change in open-grown *Q. garryana* that exhibits a convex-up profile throughout the growing season (Gould et al. 2011). This is a common trend in ring-porous species (Lei et al. 1996) and oaks from around the world (Maertens 2008). Sapflow remains high after sapwood growth stops (compare Figs. 6 and 8), leading us to propose that assimilation efficiency may decrease or that a reallocation of photosynthates from sapwood to fruit production and roots occurs throughout the growing season. The October radial increase is due primarily to tissue rehydration, as the sapwood reaches its lowest potential at the end of the summer and swells in response to early wet-season rains.

The diurnal patterns in Fig. 9 show sinusoidal shrinking and swelling of the sapwood, cambium, and inner bark. Recharge of stored water occurs when the radial size increases from late afternoon to pre-dawn, whereas depletion of stored water occurs as the radial size decreases

from pre-dawn to late afternoon. This pattern leads to the inference that stored water supplements the transpiration stream during the day at times of high sapflow and low Ψ . Phillips et al. (2003b) similarly found that *Q. garryana* tissue between the bole and crown was a net source of water for transpiration in the late morning and early afternoon, during times of maximum solar radiation, and that in the late afternoon to early evening this region was a net sink of water. They also found that the reliance on stored water approximately doubled from the early to late season, consistent with our observations in Fig. 9 of increasing diurnal amplitudes.

Volumes of stored water in the tree

We can estimate minimum daily trunk water storage by assuming the $\sim 60 \mu\text{m}$ average diurnal radial change in sapwood, cambium, and inner bark of trees (Fig. 9) is entirely due to the gain and loss of liquid water. A trunk height of 5 m for a 20 cm diameter tree (similar to the smaller trees in this study) results in daily water gain and loss of 0.2, and 1.2 L for a 10 m tall trunk and a 65 cm diameter tree (approximately the largest in this study). This does not include trunk water gain and loss that does not result in a volumetric dilation or any heartwood water storage, and only roughly approximates the trunk volume and does not include the crown stem network. We can also calculate the daily stored water in leaves. We consider a 20 cm diameter tree, with a crown radius of 4 m and an assumed leaf area index of 3. The average leaf dry mass and leaf mass/area of Table 4 results in $\sim 40,000$ leaves. Given the average daily shoot Ψ change from pre-dawn to mid-day of 1.6 MPa (Fig. 3, and we note that the diurnal leaf change would be higher), and an average leaf $\Delta H_2O_{\text{mass}}/\Delta\Psi$ before the TLP across all leaves of 0.019 g/MPa from the PV curves (available in Data S1), we estimate a daily leaf water storage of 1.3 L. A tree with a 7 m crown radius and leaf area index of 4 would have 170,000 leaves that lose 5.2 L daily. Diurnal dehydration of leaves can therefore constitute a significant fraction of the stored water contribution to transpiration—in this case, comparable to our conservative estimate of trunk sapwood contribution. If all nighttime sapflow went exclusively to tissue rehydration rather than transpiration, stored water would contribute $\sim 20\text{--}30\%$ of

the daily transpiration stream, based on the integral of diurnal sapflow curves in Fig. 6. This rehydration–transpiration partitioning estimate is not unreasonable; in a study of *Q. douglasii*, Fisher et al. (2007) found that ~70% of nocturnal sapflow went to rehydration.

Implications for competition with P. menziesii

How will the *P. menziesii* that have invaded oak savanna and woodlands fare relative to *Q. garryana* under continued warming in the 21st century? *Q. garryana* resilience, or the ability to persist in the face of climatic perturbation, hinges strongly on its water-limitation tolerance relative to *P. menziesii*. Although there is some uncertainty in climate models, mean annual temperature is among the most reliably predicted outputs (Rupp et al. 2013). Models predict that an atmospheric CO₂ concentration of ~750 ppm will globally raise average temperatures this century by 2.4°–5.4°C (Murphy et al. 2004), with Pacific Northwest regional models predicting similar rises (Mote and Salathé 2010). The mean temperature of the warmest month in Northwest California is expected to increase by 3°C (Kueppers et al. 2005). As dry-season temperatures increase, plants will experience greater VPDs in the growing season (Luce et al. 2016). Our study site, inhabited by mature *Q. garryana* experiencing extremely water-limited conditions that have also not been subject to significant *P. menziesii* invasion, may serve as a microcosm of a more water-limited future. We discuss the paleoclimatic and paleoecologic record, modern climate-distribution studies, and finally compare and contrast the ecophysiology of the species in light of the new findings in this study.

Paleoclimate and paleoecology

Regionally, Pinaceae pollen abundance is negatively correlated with *Quercus* pollen, and shifts in these two plant communities follow temperature changes throughout glacial and inter-glacial cycles (Heusser 2000, Poore et al. 2000). In the Quaternary, *Quercus* pollen abundance was lowest during glacial maxima, when temperatures were cool, and increased during warmer inter-glacial times (Mensing 2015). For example, in the Sierra Nevada, oak range expanded from 10,000 to 5000 yr before present, coincident with a warming climate (Byrne et al. 1991), and in the Northern

California Coast Ranges oaks reached a maximum extent between 6000 and 3500 yr before present at Clear Lake and 5000 yr before present at Tule Lake (Adam et al. 1981, West 1982, Adam and West 1983, Mensing 2005). Oaks reached a maximum extent in coastal British Columbia 7500 yr before present, when temperatures were 2°–4°C warmer (Pellatt et al. 2001, Walker and Pellatt 2003). Lucas and Lacourse (2013) show a rise of *Q. garryana* in the Gulf Islands of British Columbia between 7600 and 5500 yr before present, followed by cooler and moister conditions that coincided with the rise of modern *P. menziesii* forests. These findings are consistent with White et al.'s (2015) pollen and charcoal records in the latter half of the Holocene from the southern Cascade Range in Oregon. They found declining fire frequency and cooler, wetter conditions accompanied increases in mesophytic taxa including *Pseudotsuga*. In northern California and southern Oregon, Mohr et al. (2000) similarly found a peak in *Quercus* during the relatively warm and dry early Holocene, with subsequent dominance of *Pinaceae* in the cooler, wetter late Holocene. Thus, the paleoecologic and paleoclimatic record of western North America indicates that during early Holocene warming *Quercus* pollen in general and *Q. garryana* specifically became more abundant, with concomitant declines in *Pinaceae* in general and *P. menziesii* specifically.

Modern climate and ecology

Temperature in the 20th century increased by ~0.6°–0.8°C in the Pacific Northwest (Abatzoglou et al. 2014), resulting in detectable shifts in mortality and growth patterns. In Northwest California, temperature has increased even faster (~0.23°C per decade; LaDochy et al. 2007). Hember et al. (2017) found no sensitivity in the probability of mortality sensitivity of *Q. garryana* (from 373 plots) to higher reference evapotranspiration, whereas *P. menziesii* (5828 plots) exhibited strong positive sensitivity. McIntyre et al. (2015) found a 20th-century trend of declining large tree and increasing oak abundance across California that was primarily attributable to increases in climatic water deficit. Dynamic vegetation models that incorporate biogeographical patterns, future climate change projections, and fire disturbance predict an expansion of northern oak woodlands into Douglas fir–tanoak forest in Northwestern

California (Lenihan et al. 2003, Bodtker et al. 2009). Such models have not yet included the role of deeper moisture (e.g., rock moisture; sensu Rempe and Dietrich 2018), which is largely unquantified but may be important in mediating plant water stress. Although exact species-level mortality rates are difficult to ascertain, in general the Northern California Coast Range *Q. garryana* habitat experienced relatively little mortality and maintained higher leaf water content in the most recent California drought (Asner et al. 2016, Young et al. 2017).

Inter-annual variations in tree growth reveal finer-scale climatic sensitivity. Maertens (2008) analyzed a >100-yr climate and *Q. garryana* annual growth ring record at 18 sites spanning most of the species' geographic and climate range, and found that growth was positively correlated with moisture availability. Gildehaus et al. (2015) developed a crossdated 341-yr-long ring-width chronology of *Q. garryana*, near the center of its geographic range in the Willamette Valley of Oregon, and also observed higher growth with higher summer moisture availability. In contrast, Jordan and Vander Gugten (2012) found no significant correlation between *Q. garryana* growth rate and precipitation and temperature for most months preceding and within the growing season. Perhaps this is due to the confounding effect of greater water availability in the early growing season coinciding with waterlogged or overcast conditions that would tend to limit growth. Only one study to our knowledge has looked at colocated *Q. garryana* and *P. menziesii* climate-growth interactions: Franks (2008) found that in general both species' growth responded positively to current year precipitation and negatively to temperature across the southern mainland and Vancouver Island of British Columbia. However, *P. menziesii* growth declined more with lower precipitation and higher temperature in the driest part of the growing season, suggesting that it was more prone to drought stress than *Q. garryana*.

Pseudotsuga menziesii ecophysiological comparison

Decline in *P. menziesii* growth rates in the past century throughout the western United States appears to be specifically attributable to temperature increases that increase VPD, resulting in

stomatal closure and lower rates of carbon uptake (Restaino et al. 2016). This regional pattern is consistent with high stomatal aperture sensitivity to VPD in juvenile *P. menziesii* (Meinzer 1982) relative to *Q. garryana* (Merz et al. 2017). Data from Johnson et al. (2009) and Woodruff et al. (2007) indicate that 50% loss of leaf *K* occurs ≈ 2 MPa higher for *P. menziesii* than for *Q. garryana*. At the neighboring site to this study, with relatively higher subsurface water availability (pre-dawn water potentials typically > -2 MPa; Hahm et al. 2017b), *P. menziesii* sapflow declines significantly in the dry season (Link et al. 2014), indicating greater sensitivity to high summer VPD and declining subsurface water availability, a common observation for *P. menziesii* (Granier 1987, Moore et al. 2004). Phillips et al. (2003b) also documented much larger relative sapflow declines in *P. menziesii* than *Q. garryana* through the dry season in Washington and Oregon.

In contrast to the *Q. garryana* behavior in this study and of juveniles in Meinzer et al. (2016), *P. menziesii* maintains similar mid-day water potentials as water availability declines in the dry season (Domec et al. 2008). The TLP of *P. menziesii* (Jackson and Spomer 1979, Ritchie and Shula 1984, Woodruff et al. 2007, Johnson et al. 2009) is generally higher than the TLP of *Q. garryana* found in this study and others discussed previously. *Quercus garryana* has the highest wood specific gravity and shortest height at maturity of common Pacific Northwest tree species (Minore 1979, Davis 2005), suggesting that it may invest more in its hydraulic architecture than *P. menziesii*. Together, these differences in ecophysiological response to temperature and water availability are consistent with a suite of evolutionary tradeoffs, in which *Q. garryana* maintains hydraulic function in drier conditions than *P. menziesii*, likely at the cost of slower growth. Such a tradeoff would favor *P. menziesii* where atmospheric water demand is low and/or subsurface moisture supply is high, and *Q. garryana* in relatively xeric environments and/or where low-intensity fires are allowed to burn, limiting *P. menziesii* encroachment.

CONCLUSION

At our Sagehorn study site, thin soils and a shallow weathered-bedrock zone over an impermeable mélange bedrock lead to limited winter

water storage and thus limited growing season water availability, despite annual precipitation of ~1800 mm. Our intensive field measurements of mature *Quercus garryana* in a seasonally dry savanna and woodland in Northern California indicate that the species maintains hydraulic function in the summer growing season at extremely low water-availability conditions. Sustained high water use at low water potential is possible due to a robust hydraulic architecture, with specific adaptations such as dynamic leaf adjustment to lower the TLP and diurnal water storage and release in sapwood and leaves to compensate for high atmospheric moisture demand. We observed transpiration well after pre-dawn water potentials declined below the inferred TLP. Consequently, the common measurement of turgor loss from pressure–volume curves of rehydrated leaves may be of inadequate in predicting functional eco-physiological limits.

In comparison with data from previous studies of *Pseudotsuga menziesii*, *Q. garryana* is significantly more water-limitation tolerant. This helps explain the lack of *P. menziesii* invasion into our water-limited study area and suggests that future warming of western North America may favor *Q. garryana* persistence. Paleoclimatic and paleoecologic records of forest community composition in the Quaternary, as well as *Q. garryana* and *P. menziesii* growth and mortality patterns in response to modern climate changes and land use also suggest this outcome. Taken together, the evidence points toward *Q. garryana*'s resilience in a changing climate, provided that its extant habitat is protected from detrimental land use and—in relatively wetter areas—from the effects of fire exclusion-assisted conifer invasion.

ACKNOWLEDGMENTS

We gratefully acknowledge the generous land access and scientific enthusiasm provided by Marilyn and Jerry Russell and the Holleman family. Fieldwork could not have been completed without the help of Cameron Williams, Rikke Naesborg, Sky Lovill, Chris Wong, Collin Bode, Peter Steel, and Ilana Stein, and the work benefitted from input from David Dralle, members of the Dawson and Ackerly laboratories at UC Berkeley, and two reviewers. The National Center for Airborne Laser Mapping (NCALM) acquired the high-resolution elevation and vegetation point cloud data used in the study. This project was primarily

funded by the National Science Foundation—Eel River Critical Zone Observatory (EAR 1331940), with additional support from the University of California Natural Reserve System Mathias Grant.

LITERATURE CITED

- Abatzoglou, J. T., D. E. Rupp, and P. W. Mote. 2014. Seasonal climate variability and change in the Pacific Northwest of the United States. *Journal of Climate* 27:2125–2142.
- Adam, D. P., J. D. Sims, and C. K. Throckmorton. 1981. 130,000-yr continuous pollen record from Clear Lake, Lake County, California. *Geology* 9:373–377.
- Adam, D. P., and G. J. West. 1983. Temperature and precipitation estimates through the last glacial cycle from Clear lake, California, Pollen Data. *Science* 219:168–170.
- Allen, C. D., et al. 2010. A global overview of drought and heat-induced tree mortality reveals emerging climate change risks for forests. *Forest Ecology and Management* 259:660–684.
- Améglio, T., P. Archer, M. Cohen, C. Valancogne, F. Daudet, S. Dayau, and P. Cruziat. 1999. Significance and limits in the use of predawn leaf water potential for tree irrigation. *Plant and Soil* 207:155–167.
- Anderson, M., R. Graham, G. Alyanakian, and D. Martynn. 1995. Late summer water status of soils and weathered bedrock in a Giant Sequoia grove. *Soil Science* 160:415–422.
- Anderson, M. V., and R. L. Pasquinelli. 1984. Ecology and management of the Northern Oak Woodland Community, Sonoma County. Thesis. Sonoma State University, Rohnert Park, California, USA.
- Asner, G. P., P. G. Brodrick, C. B. Anderson, N. Vaughn, D. E. Knapp, and R. E. Martin. 2016. Progressive forest canopy water loss during the 2012–2015 California drought. *Proceedings of the National Academy of Sciences* 113:E249–E255.
- Barnhart, S. J., J. R. McBride, and P. Warner. 1996. Invasion of Northern Oak Woodlands by *Pseudotsuga menziesii* (Mirb.) Franco in the Sonoma Mountains of California. *Madroño* 43:28–45.
- Bartlett, M. K., C. Scoffoni, and L. Sack. 2012. The determinants of leaf turgor loss point and prediction of drought tolerance of species and biomes: a global meta-analysis. *Ecology Letters* 15:393–405.
- Begg, J. E., and N. C. Turner. 1970. Water potential gradients in field tobacco. *Plant Physiology* 46:343–346.
- Blackman, C. J., and T. J. Brodrick. 2011. Two measures of leaf capacitance: insights into the water transport pathway and hydraulic conductance in leaves. *Functional Plant Biology* 38:118–126.

- Blake, M. and D. L. Jones. 1974. Origin of Franciscan Melanges in Northern California. Special Publications of the Society of Economic Paleontologists and Mineralogists.
- Bodtker, K., M. G. Pellatt and A. Cannon. 2009. A bioclimatic model to assess the impact of climate change on ecosystems at risk and inform land management decisions. Parks Canada, Western and Northern Service Centre, Vancouver, Canada.
- Boyer, J. S. 1995. Measuring the water status of plants and soils. Academic Press Inc, Cambridge, Massachusetts, USA.
- Brodribb, T. J., and N. M. Holbrook. 2003. Stomatal closure during leaf dehydration, correlation with other leaf physiological traits. *Plant Physiology* 132:2166–2173.
- Burgess, S. S. O., M. A. Adams, N. C. Turner, C. R. Beverly, C. K. Ong, A. A. H. Khan, and T. M. Bleby. 2001. An improved heat pulse method to measure low and reverse rates of sap flow in woody plants. *Tree Physiology* 21:589–598.
- Byrne, R., E. Edlund, and S. Mensing. 1991. Holocene changes in the distribution and abundance of oaks in California. Pages 182–188 Proceedings of the Symposium on Oak Woodlands and Hardwood Rangeland Management. USDA Forest Service General Technical Report PSW-126.
- California Department of Forestry. 1996. California oak woodland community. California Oaks, Oakland, California, USA.
- Cannon, W. A. 1914. Specialization in vegetation and in environment in California. *The Plant World* 17:223–237.
- Christy, J. A., and E. R. Alverson. 2011. Historical vegetation of the Willamette Valley, Oregon, circa 1850. *Northwest Science* 85:93–107.
- Cloos, M. 1982. Flow melanges: numerical modeling and geologic constraints on their origin in the Franciscan subduction complex, California. *Geological Society of America Bulletin* 93:330–345.
- Cocking, M. I., J. M. Varner, and E. A. Engber. 2015. Conifer encroachment in California oak woodlands. Page Gen. Tech. Rep. PSW-GTR-251. USDA Forest Service, Washington, DC, USA.
- Cole, D. 1977. Ecosystem dynamics in the coniferous forest of the Willamette Valley, Oregon, USA. *Journal of Biogeography* 4:181–192.
- Davis, K. J. 2005. Comparison of the water relations characteristics of woody plants in western Oregon. Oregon State University, Corvallis, Oregon, USA.
- Dawson, T. E., and L. C. Bliss. 1989. Patterns of water use and the tissue water relations in the dioecious shrub, *Salix arctica*: the physiological basis for habitat partitioning between the sexes. *Oecologia* 79:332–343.
- Dawson, T. E., S. S. O. Burgess, K. P. Tu, R. S. Oliveira, L. S. Santiago, J. B. Fisher, K. A. Simonin, and A. R. Ambrose. 2007. Nighttime transpiration in woody plants from contrasting ecosystems. *Tree Physiology* 27:561–575.
- Devine, W. D., and C. A. Harrington. 2005. Root system morphology of Oregon white oak on a glacial outwash soil. *Northwest science* 79:179–188.
- Devine, W. D., and C. A. Harrington. 2006. Changes in Oregon white oak (*Quercus garryana* Dougl. ex Hook.) following release from overtopping conifers. *Trees* 20:747–756.
- Domec, J.-C., B. Lachenbruch, F. C. Meinzer, D. R. Woodruff, J. M. Warren, and K. A. McCulloh. 2008. Maximum height in a conifer is associated with conflicting requirements for xylem design. *Proceedings of the National Academy of Sciences* 105:12069–12074.
- Domec, J.-C., F. C. Meinzer, B. Lachenbruch, and J. Housset. 2007. Dynamic variation in sapwood specific conductivity in six woody species. *Tree Physiology* 27:1389–1400.
- Donovan, L. A., J. H. Richards, and M. J. Linton. 2003. Magnitude and mechanisms of disequilibrium between predawn plant and soil water potentials. *Ecology* 84:463–470.
- Dralle, D. N., W. J. Hahm, D. M. Rempe, N. J. Karst, S. E. Thompson, and W. E. Dietrich. *In press*. Quantification of the seasonal hillslope water storage that does not drive streamflow. *Hydrological Processes*.
- Dunwiddie, P. W., and J. D. Bakker. 2011. The future of restoration and management of prairie-oak ecosystems in the Pacific Northwest. *Northwest Science* 85:83–92.
- Dunwiddie, P. W., J. D. Bakker, M. Almaguer-Bay, and C. B. Sprenger. 2011. Environmental history of a Garry Oak/Douglas-Fir Woodland on Waldron Island, Washington. *Northwest Science* 85:130–140.
- Engber, E. A., and J. M. Varner. 2012. Predicting Douglas-fir sapling mortality following prescribed fire in an encroached grassland. *Restoration Ecology* 20:665–668.
- Erickson, W. R. 1996. Classification and interpretation of garry oak (*Quercus garryana*) plant communities and ecosystems in southwestern British Columbia. Thesis. University of Victoria, Victoria, British Columbia, Canada.
- Farrell, C., C. Szota, and S. K. Arndt. 2017. Does the turgor loss point characterize drought response in dryland plants? *Plant, Cell & Environment* 40:1500–1511.
- Fisher, J. B., D. D. Baldocchi, L. Misson, T. E. Dawson, and A. H. Goldstein. 2007. What the towers don't

- see at night: nocturnal sap flow in trees and shrubs at two AmeriFlux sites in California. *Tree Physiology* 27:597–610.
- Foley, J. A., et al. 2005. Global consequences of land use. *Science* 309:570–574.
- Franklin, J., and C. Dyrness. 1973. Page 427 Natural vegetation of Oregon and Washington. Gen. Tech. Rep. USDA Forest Service, Washington, DC, USA.
- Franks, J. 2008. Competitive dynamics in a mixed Garry oak/Douglas-fir stand based on tree ring analysis. Thesis. University of Guelph (Canada), Guelph, Ontario, Canada.
- Fuchs, M. A. 2001. Towards a recovery strategy for Garry oak and associated ecosystems in Canada: ecological assessment and literature review. *Environment Canada, Pacific and Yukon Region*.
- Gaines, K. P., J. W. Stanley, F. C. Meinzer, K. A. McCulloh, D. R. Woodruff, W. Chen, T. S. Adams, H. Lin, and D. M. Eissenstat. 2016. Reliance on shallow soil water in a mixed-hardwood forest in central Pennsylvania. *Tree Physiology* 36:444–458.
- Gedalof, Z., M. Pellatt, and D. J. Smith. 2006. From prairie to forest: three centuries of environmental change at Rocky Point, Vancouver Island, British Columbia. *Northwest Science* 80:34–46.
- Gildehaus, S., K. Arabas, E. Larson, and K. Copes-Gerbitz. 2015. The dendroclimatological potential of Willamette Valley *Quercus garryana*. *Tree-Ring Research* 71:13–23.
- Gilligan, L. A., and P. S. Muir. 2011. Stand structures of Oregon white oak woodlands, regeneration, and their relationships to the environment in Southwestern Oregon. *Northwest Science* 85:141–158.
- Gould, P. J., C. A. Harrington, and W. D. Devine. 2011. Growth of Oregon White Oak (*Quercus garryana*). *Northwest Science* 85:159–171.
- Granier, A. 1987. Evaluation of transpiration in a Douglas-fir stand by means of sap flow measurements. *Tree Physiology* 3:309–320.
- Griffin, J. R. 1973. Xylem sap tension in three woodland oaks of Central California. *Ecology* 54:152–159.
- Griffin, J. R., and W. B. Critchfield. 1972. The distribution of forest trees in California. Res. Paper PSW-RP-82. Pacific Southwest Forest and Range Experiment Station, Forest Service, U.S. Department of Agriculture, Berkeley, California, USA.
- Hahm, W. J., W. E. Dietrich, and T. E. Dawson. 2017a. Progressive depletion of stable isotopes recorded in a Mediterranean oak (*Q. garryana*) as a shallow saturated water source drains, leaving behind tightly held rock moisture. *Isotopes Switzerland 2017 Conference Proceedings*. Verità, Ascona.
- Hahm, W. J., W. E. Dietrich, D. M. Rempe, D. N. Dralle, T. E. Dawson, S. Lovill, and A. Bryk. 2017b. The influence of Critical Zone structure on runoff paths, seasonal water storage, and ecosystem composition (invited). *In AGU Fall Meeting Conference Proceedings*. American Geophysical Union, New Orleans, Louisiana, USA.
- Hahm, W. J., D. N. Dralle, S. Lovill, J. Rose, T. E. Dawson, and W. E. Dietrich. 2017c. Exploratory Tree Survey (2016 - Eel River Critical Zone Observatory - Sagehorn - Central Belt Melange, Franciscan Complex, Northern California Coast Ranges, USA). HydroShare. <https://doi.org/10.4211/hs.7881821a5c0e4ae3822b96a59f4bf8b6>
- Hastings, M. S., S. Barnhart, and J. R. McBride. 1997. Restoration management of northern oak woodlands. USDA Forest Service, Washington, DC, USA.
- Hellkvist, J., G. P. Richards, and P. G. Jarvis. 1974. Vertical gradients of water potential and tissue water relations in Sitka spruce trees measured with the pressure chamber. *Journal of Applied Ecology* 11:637–667.
- Hember, R. A., W. A. Kurz, and N. C. Coops. 2017. Relationships between individual-tree mortality and water-balance variables indicate positive trends in water stress-induced tree mortality across North America. *Global Change Biology* 23:1691–1710.
- Heusser, L. E. 2000. Rapid oscillations in western North America vegetation and climate during oxygen isotope stage 5 inferred from pollen data from Santa Barbara Basin (Hole 893A). *Palaeogeography, Palaeoclimatology, Palaeoecology* 161:407–421.
- Holdridge, L. R. 1947. Determination of world plant formations from simple climatic data. *Science* 105:367–368.
- Jackson, P. A., and G. G. Spomer. 1979. Biophysical adaptations of four western conifers to habitat water conditions. *Botanical Gazette* 140:428–432.
- Jayko, A. S., M. C. Blake, R. J. McLaughlin, H. N. Ohlin, S. D. Ellen, and H. M. Kelsey. 1989. Reconnaissance geologic map of the Covelo 30- by 60-minute Quadrangle, Northern California. United States Geological Survey, Denver, Colorado, USA.
- Johnson, D. M., K. A. McCulloh, D. R. Woodruff, and F. C. Meinzer. 2012. Evidence for xylem embolism as a primary factor in dehydration-induced declines in leaf hydraulic conductance. *Plant, Cell & Environment* 35:760–769.
- Johnson, D. M., D. R. Woodruff, K. A. McCulloh, and F. C. Meinzer. 2009. Leaf hydraulic conductance, measured in situ, declines and recovers daily: leaf hydraulics, water potential and stomatal conductance in four temperate and three tropical tree species. *Tree Physiology* 29:879–887.

- Joly, R. J., and J. B. Zaerr. 1987. Alteration of cell-wall water content and elasticity in Douglas-Fir during periods of water deficit. *Plant Physiology* 83:418–422.
- Jones, D. P., and R. C. Graham. 1993. Water-holding characteristics of weathered granitic rock in chaparral and forest ecosystems. *Soil Science Society of America Journal* 57:256–261.
- Jordan, D. A., and K. Vander Gugten. 2012. Dendrochronological potential of *Quercus garryana*, Saltspring Island, British Columbia. *Tree-Ring Research* 68:51–58.
- Kelly, J. 2016. Physiological responses to drought in healthy and stressed trees: a comparison of four species in Oregon, USA. Lund University, Lund, Sweden.
- Kubiske, M. E., and M. D. Abrams. 1990. Pressure-volume relationships in non-rehydrated tissue at various water deficits. *Plant, Cell & Environment* 13:995–1000.
- Kueppers, L. M., M. A. Snyder, L. C. Sloan, E. S. Zavaleta, and B. Fulfrost. 2005. Modeled regional climate change and California endemic oak ranges. *Proceedings of the National Academy of Sciences* 102:16281–16286.
- LaDochy, S., R. Medina, and W. Patzert. 2007. Recent California climate variability: spatial and temporal patterns in temperature trends. *Climate Research* 33:159–169.
- Langenheim, V. E., R. C. Jachens, C. M. Wentworth, and R. J. McLaughlin. 2013. Previously unrecognized regional structure of the Coastal Belt of the Franciscan Complex, northern California, revealed by magnetic data. *Geosphere* 9:1514–1529.
- Lei, H., M. R. Milota, and B. L. Gartner. 1996. Between- and within-tree variation in the anatomy and specific gravity of wood in Oregon White Oak (*Quercus Garryana* Dougl.). *IAWA Journal* 17:445–461.
- Lenihan, J. M., R. Drapek, D. Bachelet, and R. P. Neilson. 2003. Climate change effects on vegetation distribution, carbon, and fire in California. *Ecological Applications* 13:1667–1681.
- Lewis, D. C., and R. H. Burgy. 1964. The relationship between oak tree roots and groundwater in fractured rock as determined by tritium tracing. *Journal of Geophysical Research* 69:2579–2588.
- Link, P., K. Simonin, H. Maness, J. Oshun, T. Dawson, and I. Fung. 2014. Species differences in the seasonality of evergreen tree transpiration in a Mediterranean climate: analysis of multiyear, half-hourly sap flow observations. *Water Resources Research* 50:1869–1894.
- Little, E. L. 1971. Atlas of United States trees. U.S. Department of Agriculture, Forest Service, Washington, D.C., USA.
- Loarie, S. R., P. B. Duffy, H. Hamilton, G. P. Asner, C. B. Field, and D. D. Ackerly. 2009. The velocity of climate change. *Nature* 462:1052–1055.
- Lovill, S., W. J. Hahm, and W. E. Dietrich. *In press*. Drainage from the critical zone: lithologic controls on the persistence and spatial extent of wetted channels during the summer dry season. *Water Resources Research*. <http://doi.org/10.1029/2017WR021903>
- Lucas, J. D., and T. Lacourse. 2013. Holocene vegetation history and fire regimes of *Pseudotsuga menziesii* forests in the Gulf Islands National Park Reserve, southwestern British Columbia, Canada. *Quaternary Research* 79:366–376.
- Luce, C. H., J. M. Vose, N. Pederson, J. Campbell, C. Millar, P. Kormos, and R. Woods. 2016. Contributing factors for drought in United States forest ecosystems under projected future climates and their uncertainty. *Forest Ecology and Management* 380:299–308.
- Maertens, T. B. 2008. The growth-climate relationship of Oregon white oak (*Quercus garryana*). Thesis. University of Guelph (Canada), Guelph, Ontario, Canada.
- Marlon, J. R., P. J. Bartlein, C. Carcaillet, D. G. Gavin, S. P. Harrison, P. E. Higuera, F. Joos, M. J. Power, and I. C. Prentice. 2008. Climate and human influences on global biomass burning over the past two millennia. *Nature Geoscience* 1:697–702.
- Marshall, D. C. 1958. Measurement of sap flow in conifers by heat transport. *Plant Physiology* 33:385–396.
- Marshall, J. G., and E. B. Dumbroff. 1999. Turgor regulation via cell wall adjustment in white spruce. *Plant Physiology* 119:313–320.
- Martínez-Vilalta, J., and N. Garcia-Forner. 2017. Water potential regulation, stomatal behaviour and hydraulic transport under drought: deconstructing the iso/anisohydric concept. *Plant, Cell & Environment* 40:962–976.
- McCune, J. L., M. G. Pellatt, and M. Vellend. 2013. Multidisciplinary synthesis of long-term human-ecosystem interactions: a perspective from the Garry oak ecosystem of British Columbia. *Biological Conservation* 166:293–300.
- McDadi, O., and R. J. Hebda. 2008. Change in historic fire disturbance in a Garry oak (*Quercus garryana*) meadow and Douglas-fir (*Pseudotsuga menziesii*) mosaic, University of Victoria, British Columbia, Canada: a possible link with First Nations and Europeans. *Forest Ecology and Management* 256:1704–1710.
- McDowell, N., et al. 2008. Mechanisms of plant survival and mortality during drought: Why do some plants survive while others succumb to drought? *New Phytologist* 178:719–739.

- McIntyre, P. J., J. H. Thorne, C. R. Dolanc, A. L. Flint, L. E. Flint, M. Kelly, and D. D. Ackerly. 2015. Twentieth-century shifts in forest structure in California: denser forests, smaller trees, and increased dominance of oaks. *Proceedings of the National Academy of Sciences* 112:1458–1463.
- McLaughlin, R. J., W. V. Sliter, N. O. Frederiksen, W. P. Harbert, and D. S. McCulloch. 1994. Plate motions recorded in tectonostratigraphic terranes of the Franciscan complex and evolution of the Mendocino triple junction, northwestern California. US Geological Survey, Denver, Colorado, USA.
- Meinzer, F. C. 1982. The effect of vapor pressure on stomatal control of gas exchange in Douglas fir (*Pseudotsuga menziesii*) saplings. *Oecologia* 54:236–242.
- Meinzer, F. C., B. J. Bond, J. M. Warren, and D. R. Woodruff. 2005. Does water transport scale universally with tree size? *Functional Ecology* 19:558–565.
- Meinzer, F. C., P. W. Rundel, M. R. Sharifi, and E. T. Nilson. 1986. Turgor and osmotic relations of the desert shrub *Larrea tridentata*. *Plant, Cell & Environment* 9:467–475.
- Meinzer, F. C., D. R. Woodruff, D. E. Marias, K. A. McCulloch, and S. Sevanto. 2014. Dynamics of leaf water relations components in co-occurring iso- and anisohydric conifer species. *Plant, Cell & Environment* 37:2577–2586.
- Meinzer, F. C., D. R. Woodruff, D. E. Marias, D. D. Smith, K. A. McCulloch, A. R. Howard, and A. L. Magedman. 2016. Mapping ‘hydroscares’ along the iso- to anisohydric continuum of stomatal regulation of plant water status. *Ecology Letters* 19:1343–1352.
- Mensing, S. 2005. The history of oak woodlands in California, part I: the paleoecologic record. *California Geographer* 45:1–38.
- Mensing, S. 2015. The paleohistory of California Oaks. *In* Proceedings of the seventh California oak symposium: managing oak woodlands in a dynamic world. USDA Forest Service, Washington, DC, USA.
- Merz, M., R. Donahue, and M. Poulson. 2017. Physiological response of Garry oak (*Quercus garryana*) seedlings to drought. *Northwest Science* 91:140–159.
- Miller, C. 2002. Management requirements for conservation of Garry oak and associated ecosystems in British Columbia. Thesis Royal Roads University (Canada), Victoria, British Columbia, Canada.
- Miller, G. R., X. Chen, Y. Rubin, S. Ma, and D. D. Baldocchi. 2010. Groundwater uptake by woody vegetation in a semiarid oak savanna. *Water Resources Research* 46:W10503.
- Minore, D. 1979. Comparative autecological characteristics of northwestern tree species—a literature review. Gen. Tech. Rep. USDA Forest Service, Washington, DC, USA.
- Mitchell, P. J., E. J. Veneklaas, H. Lambers, and S. S. O. Burgess. 2008. Leaf water relations during summer water deficit: differential responses in turgor maintenance and variation in leaf structure among different plant communities in south-western Australia. *Plant, Cell & Environment* 31:1791–1802.
- Mohr, J. A., C. Whitlock, and C. N. Skinner. 2000. Post-glacial vegetation and fire history, eastern Klamath Mountains, California, USA. *The Holocene* 10:587–601.
- Moore, G. W., B. J. Bond, J. A. Jones, N. Phillips, and F. C. Meinzer. 2004. Structural and compositional controls on transpiration in 40- and 450-year-old riparian forests in western Oregon, USA. *Tree Physiology* 24:481–491.
- Mote, P. W., and E. P. Salathé. 2010. Future climate in the Pacific Northwest. *Climatic Change* 102:29–50.
- Murphy, J. M., D. M. H. Sexton, D. N. Barnett, G. S. Jones, M. J. Webb, M. Collins, and D. A. Stainforth. 2004. Quantification of modelling uncertainties in a large ensemble of climate change simulations. *Nature* 430:768–772.
- Parks Canada. 2006a. Recovery strategy for multi-species at risk in Garry oak woodlands in Canada. Parks Canada, Ottawa, Canada.
- Parks Canada. 2006b. Recovery strategy for multi-species at risk in maritime meadows associated with Garry oak ecosystems in Canada. Parks Canada, Ottawa, Canada.
- Pellatt, M. G., and Z. Gedalof. 2014. Environmental change in Garry oak (*Quercus garryana*) ecosystems: the evolution of an eco-cultural landscape. *Biodiversity and Conservation* 23:2053–2067.
- Pellatt, M. G., R. J. Hebda, and R. W. Mathewes. 2001. High-resolution Holocene vegetation history and climate from Hole 1034B, ODP leg 169S, Saanich Inlet, Canada. *Marine Geology* 174:211–222.
- Pellatt, M. G., M. M. McCoy, and R. W. Mathewes. 2015. Paleoecology and fire history of Garry oak ecosystems in Canada: implications for conservation and environmental management. *Biodiversity and Conservation* 24:1621–1639.
- Phillips, N., B. J. Bond, N. G. McDowell, M. G. Ryan, and A. Schauer. 2003a. Leaf area compounds height-related hydraulic costs of water transport in Oregon White Oak trees. *Functional Ecology* 17:832–840.
- Phillips, N. G., M. G. Ryan, B. J. Bond, N. G. McDowell, T. M. Hinckley, and J. Čermák. 2003b. Reliance on stored water increases with tree size in three

- species in the Pacific Northwest. *Tree Physiology* 23:237–245.
- Poore, R. Z., H. J. Dowsett, J. A. Barron, L. Heusser, A. C. Ravelo, and A. Mix. 2000. Multiproxy record of the last interglacial (MIS 5e) off central and northern California, U.S.A., from Ocean Drilling Program sites 1018 and 1020. USGS Numbered Series, U.S. Geological Survey, Reston, Virginia, USA.
- Porporato, A., F. Laio, L. Ridolfi, and I. Rodriguez-Iturbe. 2001. Plants in water-controlled ecosystems: active role in hydrologic processes and response to water stress. *Advances in Water Resources* 24:725–744.
- Reed, L. J., and N. G. Sugihara. 1987. Northern oak woodlands: Ecosystem in jeopardy or is it already too late? USDA Forest Service General Technical Report, Pacific Southwest Forest and Range Experiment Station, Berkeley, California, USA.
- Rempe, D. M., and W. E. Dietrich. 2018. Direct observations of rock moisture, a hidden component of the hydrologic cycle. *Proceedings of the National Academy of Sciences* 115:2664–2669.
- Restaino, C. M., D. L. Peterson, and J. Littell. 2016. Increased water deficit decreases Douglas fir growth throughout western US forests. *Proceedings of the National Academy of Sciences* 113: 9557–9562.
- Ritchie, G. A., and R. G. Shula. 1984. Seasonal changes of tissue-water relations in shoots and root systems of Douglas-fir seedlings. *Forest Science* 30:538–548.
- Rittiman Jr., C., and T. Thorson. 2001. Soil survey of Mendocino County. California, Western Part, Mendocino County Resource Conservation District.
- Rupp, D. E., J. T. Abatzoglou, K. C. Hegewisch, and P. W. Mote. 2013. Evaluation of CMIP5 20th century climate simulations for the Pacific Northwest USA. *Journal of Geophysical Research: Atmospheres* 118:2013JD020085.
- Smith, S. J., J. Edmonds, C. A. Hartin, A. Mundra, and K. Calvin. 2015. Near-term acceleration in the rate of temperature change. *Nature Climate Change* 5:333–336.
- Snyder, R. 2005. The ASCE standardized reference evapotranspiration equation. ASCE, Reston, Virginia, USA.
- Sprague, F. L., and H. P. Hansen. 1946. Forest succession in the McDonald Forest, Willamette Valley, Oregon. *Northwest science* 20:89–98.
- Stein, W. 1990. *Quercus garryana* Dougl. ex Hook. Oregon White Oak. in R. M. Burns and B. H. Honkala, tech. coords. *Silvics of North America, Volume II: Hardwoods*. USDA Forest Service, Washington, D.C.
- Sugihara, N. G., J. van Wagtenonk, and J. Fites-Kaufman. 2006. Fire as an ecological process. Page Fire in California's Ecosystems. University of California Press, Berkeley, California, USA.
- Thilenius, J. F. 1968. The *Quercus garryana* forests of the Willamette Valley, Oregon. *Ecology* 49:1124–1133.
- Thompson, J. 2007. Move over, Douglas-fir: Oregon white oaks need room to grow. USDA Forest Service, Portland, Oregon, USA.
- Thysell, D. R., and A. B. Carey. 2001. *Quercus garryana* communities in the Puget Trough, Washington. *Northwest Science* 75:219–235.
- Ugolini, F. C., and A. K. Schlichte. 1973. The effect of holocene environmental changes on selected western Washington soils. *Soil Science* 116:218–227.
- US Forest Service. 2016. New aerial survey identifies more than 100 million dead trees in California. USDA Office of Communications, Vallejo, California, USA.
- Walker, I. R., and M. G. Pellatt. 2003. Climate change in Coastal British Columbia—A paleoenvironmental perspective. *Canadian Water Resources Journal/Revue canadienne des ressources hydriques* 28:531–566.
- Warton, D. I., I. J. Wright, D. S. Falster, and M. Westoby. 2006. Bivariate line-fitting methods for allometry. *Biological Reviews* 81:259–291.
- West, G. J. 1982. Pollen analysis of sediments from Tule Lake: a record of Holocene vegetation/climatic changes in the Mendocino National Forest, California. In *Proceedings, Symposium of Holocene Climate and Archeology of California's Coast and Desert*. Special Publication, Anthropology Department, San Diego State University, San Diego, California, USA.
- West, A. G., T. E. Dawson, E. C. February, G. F. Midgley, W. J. Bond, and T. L. Aston. 2012. Diverse functional responses to drought in a Mediterranean-type shrubland in South Africa. *New Phytologist* 195:396–407.
- White, A., C. Briles, and C. Whitlock. 2015. Postglacial vegetation and fire history of the southern Cascade Range, Oregon. *Quaternary Research* 84:348–357.
- Williams, C. B., R. Reese Næsborg, T. E. Dawson, and M. Cavaleri. 2017. Coping with gravity: the foliar water relations of giant sequoia. *Tree Physiology* 37:1312–1326.
- Woodruff, D. R., K. A. McCulloh, J. M. Warren, F. C. Meinzer, and B. Lachenbruch. 2007. Impacts of tree height on leaf hydraulic architecture and stomatal control in Douglas-fir. *Plant, Cell & Environment* 30:559–569.
- Woodward, F. I. 1987. *Climate and plant distribution*. Cambridge University Press, Cambridge, UK.
- Xu, L., and D. D. Baldocchi. 2003. Seasonal trends in photosynthetic parameters and stomatal conductance

- of blue oak (*Quercus douglasii*) under prolonged summer drought and high temperature. *Tree Physiology* 23:865–877.
- Young, D. J. N., J. T. Stevens, J. M. Earles, J. Moore, A. Ellis, A. L. Jirka, and A. M. Latimer. 2017. Long-term climate and competition explain forest mortality patterns under extreme drought. *Ecology Letters* 20:78–86.
- Zack, S., M. K. Chase, G. R. Geupel, and D. Stralberg. 2005. The oak woodland bird conservation plan: a strategy for protecting and managing oak woodland habitats and associated birds in California. Pages 20–24 *in* Bird conservation implementation and integration in the Americas. USDA Forest Service, Washington, DC, USA.
- Zweifel, R., L. Zimmermann, F. Zeugin, and D. M. Newbery. 2006. Intra-annual radial growth and water relations of trees: implications towards a growth mechanism. *Journal of Experimental Botany* 57:1445–1459.

DATA AVAILABILITY

Time-series data for this project are available at <http://sensor.berkeley.edu/>. The accompanying datasets referenced as Data S1–S4 contain pressure–volume curve data, leaf hydraulic conductance data, pre-dawn and mid-day water potential data, and leaf vs. stem water potential data, respectively.

SUPPORTING INFORMATION

Additional Supporting Information may be found online at: <http://onlinelibrary.wiley.com/doi/10.1002/ecs2.2218/full>